

Universal Parameterization of Absorption Cross Sections

R. K. Tripathi
Southern Illinois University • Carbondale, Illinois

Francis A. Cucinotta and John W. Wilson
Langley Research Center • Hampton, Virginia

Available electronically at the following URL address: <http://techreports.larc.nasa.gov/ltrs/ltrs.html>

Printed copies available from the following:

NASA Center for AeroSpace Information
800 Elkridge Landing Road
Linthicum Heights, MD 21090-2934
(301) 621-0390

National Technical Information Service (NTIS)
5285 Port Royal Road
Springfield, VA 22161-2171
(703) 487-4650

Abstract

This paper presents a simple universal parameterization of total reaction cross sections for any system of colliding nuclei that is valid for the entire energy range from a few AMeV to a few AGeV. The universal picture presented here treats proton-nucleus collision as a special case of nucleus-nucleus collision, where the projectile has charge and mass number of one. The parameters are associated with the physics of the collision system. In general terms, Coulomb interaction modifies cross sections at lower energies, and the effects of Pauli blocking are important at higher energies. The agreement between the calculated and experimental data is better than all earlier published results.

Introduction

Transportation of energetic ions in bulk matter is of direct interest in several areas (ref. 1), including shielding against ions originating from either space radiations or terrestrial accelerators, cosmic ray propagation studies in a galactic medium, or radiobiological effects resulting from the workplace or clinical exposures. For carcinogenesis, terrestrial radiation therapy, and radiobiological research, knowledge of the beam composition and interactions is necessary to properly evaluate the effects on human and animal tissues. For proper assessment of radiation exposures, both reliable transport codes and accurate input parameters are needed.

One such important input is the total reaction (σ_R) cross section, defined as the total (σ_T) minus the elastic (σ_{el}) cross sections for two colliding ions:

$$\sigma_R = \sigma_T - \sigma_{el} \quad (1)$$

In view of its importance, the total reaction cross section has been extensively studied both theoretically (refs. 1–14) and experimentally (refs. 15–24) for the past five decades. A detailed list of references is given in references 1, 13, and 16. Empirical prescriptions have been developed (refs. 2–4, 10, 11, and 13) for the total reaction cross sections working in various energy ranges and combination of interacting ions. The present model works in all energy ranges with uniform accuracy for any combination of interacting ions, including proton-nucleus collisions, and is more accurate than earlier reported empirical models (ref. 10), which were accurate above 100 AMeV but showed large errors up to 25 percent at lower energies.

Model Description

Most of the empirical models approximate the total reaction cross section of Bradt-Peters form with

$$\sigma_R = \pi r_0^2 \left(A_P^{1/3} + A_T^{1/3} - \delta \right)^2 \quad (2)$$

where r_0 is energy-independent, δ is either an energy-independent or energy-dependent parameter, and A_P and A_T are the projectile and target mass numbers, respectively. This form of parameterization works nicely for higher energies. However, for lower energies, Coulomb interaction becomes important and modifies reaction cross sections significantly. In addition, strong absorption models suggest energy dependence of the interaction radius. Incorporating these effects, and other effects discussed later in the text, we propose the following form for the reaction cross section:

$$\sigma_R = \pi r_0^2 \left(A_P^{1/3} + A_T^{1/3} + \delta_E \right)^2 \left(1 - \frac{B}{E_{cm}} \right) \quad (3)$$

where $r_0 = 1.1$ fm, and E_{cm} is the colliding system center of mass energy in MeV. The last term in equation (3) is the Coulomb interaction term, which modifies the cross section at lower energies and becomes less important as the energy increases (typically after several tens of AMeV). In equation (3), B is the energy-dependent Coulomb interaction barrier (factor on right side of eq. (3)) and is given by

$$B = \frac{1.44 Z_P Z_T}{R} \quad (4)$$

where Z_P and Z_T are the atomic numbers of the projectile and target, respectively, and R , the distance for evaluating the Coulomb barrier height, is

$$R = r_P + r_T + \frac{1.2 \left(A_P^{1/3} + A_T^{1/3} \right)}{E_{cm}^{1/3}} \quad (5)$$

where r_i is equivalent sphere radius and is related to the $r_{rms,i}$ radius by

$$r_i = 1.29 r_{rms,i} \quad (6)$$

with ($i = P, T$).

The energy dependence in the reaction cross section at intermediate and higher energies results mainly from two effects—transparency and Pauli blocking. This energy dependence is taken into account in δ_E , which is given by

$$\delta_E = 1.85S + \left(0.16S/E_{cm}^{1/3}\right) - C_E + [0.91(A_T - 2Z_T)Z_P/(A_TA_P)] \quad (7)$$

where S is the mass asymmetry term given by

$$S = \frac{A_P^{1/3}A_T^{1/3}}{A_P^{1/3} + A_T^{1/3}} \quad (8)$$

and is related to the volume overlap of the collision system. The last term on the right side of equation (7) accounts for the isotope dependence of the reaction cross section. The term C_E is related to both the transparency and Pauli blocking and is given by

$$C_E = D[1 - \exp(-E/40)] - 0.292\exp(-E/792) \times \cos\left(0.229E^{0.453}\right) \quad (9)$$

where the collision kinetic energy E is in units of AMeV. Here, D is related to the density dependence of the colliding system, scaled with respect to the density of the $^{12}\text{C} + ^{12}\text{C}$ colliding system:

$$D = 1.75 \frac{\rho_{A_P} + \rho_{A_T}}{\rho_{A_C} + \rho_{A_C}} \quad (10)$$

The density of a nucleus is calculated in the hard-sphere model. Important physics is associated with constant D . In effect, D simulates the modifications of the reaction cross sections caused by Pauli blocking. The Pauli blocking effect, which has not been taken into account in other empirical calculations, is being introduced here for the first time. Introduction of the Pauli blocking effect helps present a universal picture of the reaction cross sections.

At lower energies (below several tens of AMeV) where the overlap of interacting nuclei is small (and where the Coulomb interaction modifies the reaction cross sections significantly), the modifications of the cross sections caused by Pauli blocking are small and gradually play an increasing role as the energy increases, which leads to higher densities where Pauli blocking becomes increasingly important. Interestingly enough,

for the proton-nucleus case, because there is not much compression effect, a single constant value of $D = 2.05$ gives very good results for all proton-nucleus collisions. For alpha-nucleus collisions, where there is a little compression, the best value of D is given by

$$D = 2.77 - \left(8.0 \times 10^{-3}A_T\right) + \left(1.8 \times 10^{-5}A_T^2\right) - 0.8/\{1 + \exp[(250 - E)/75]\} \quad (11)$$

For lithium nuclei, because of the “halos” (ref. 21), compression is less; therefore, the Pauli blocking effect is less important. A reduced value of $D/3$ gives better results for the reaction cross sections at the intermediate and higher energies.

There are no adjustable parameters in the model except that, for proton-nucleus collisions, this method of calculating the Coulomb interaction barrier underestimates its value for the very light closed-shell nuclei of alpha and carbon, which are very tightly bound and, therefore, compact. Consequently, for these two cases, the Coulomb barrier should be increased by a factor of 27 and 3.5, respectively, for a better fit.

Results and Conclusions

Figures 1–45 show the plots of available results for proton-nucleus, alpha-nucleus, and nucleus-nucleus collisions. Figures 6 and 18 also show comparisons with reference 10. The data set used for figures 1–5 was collected from references 15 and 23 and, for figures 6–14, was obtained from references 16, 17, 22, and 23. Extensive data available for a C + C system (fig. 18) were taken from references 16, 17, 23, and 24. For the remaining figures, data were collected from the compilation of data sets from references 9 and 16–20. The agreement with experiment is excellent and is better than all other empirical models reported earlier, which is particularly important in view of the fact that the agreement is excellent throughout the whole energy range—up to a few AGeV. We notice, again, that at the lower energy end, the cross sections are modified by the Coulomb interaction, and at the intermediate and high energy end, Pauli blocking effects become increasingly important. It will be interesting to see how the model compares with the new experimental data as and when these become available.

NASA Langley Research Center
Hampton, VA 23681-0001
December 17, 1996

References

1. Wilson, John W.; Townsend, Lawrence W.; Schimmerling, Walter; Khandelwal, Govind S.; Khan, Ferdous; Nealy, John E.; Cucinotta, Francis A.; Simonsen, Lisa C.; Shinn, Judy L.; and Norbury, John W.: *Transport Methods and Interactions for Space Radiations*. NASA RP-1257, 1992.
2. Bass, Reiner: *Nuclear Reactions With Heavy Ions*. Springer-Verlag, 1980.
3. Bradt, H. L.; and Peters, B.: The Heavy Nuclei of the Primary Cosmic Radiation. *Phys. Rev.*, second ser., vol. 77, no. 1, Jan. 1, 1950, pp. 54–70.
4. Karol, Paul J.: Nucleus-Nucleus Reaction Cross Sections at High Energies: Soft-Spheres Model. *Phys. Rev. C*, vol. 11, no. 4, Apr. 1975, pp. 1203–1209.
5. Glauber, R. J.: *High-Energy Collision Theory. Lectures in Theoretical Physics, Volume I*, Wesley E. Brittin and Lita G. Dunham, eds., Interscience Publ., Inc., 1959, pp. 315–414.
6. Wilson, John W.: Composite Particle Reaction Theory. Ph.D. Diss., College of William and Mary, June 1975.
7. Wilson, J. W.; and Townsend, L. W.: An Optical Model for Composite Nuclear Scattering. *Canadian J. Phys.*, vol. 59, no. 11, 1981, pp. 1569–1576.
8. Ernst, David J.: Total Reaction Cross Sections and the Matter Density of Finite Nuclei. *Phys. Rev. C*, vol. 19, no. 3, Mar. 1979, pp. 896–904.
9. Gupta, S. K.; and Shukla, P.: Trajectory Modifications in the Glauber Model for Heavy Ions. *Phys. Rev. C*, vol. 52, no. 6, Dec. 1995, pp. 3212–3216 and references.
10. Townsend, L. W.; and Wilson, J. W.: Energy-Dependent Parameterization of Heavy-Ion Absorption Cross Sections. *Radiat. Res.*, vol. 106, 1986, pp. 283–287.
11. Shen, Wen-Qing; Wang, Bing; Feng, Jun; Zhan, Wen-Long; Zhu, Yong-Tai; and Feg, En-Pu: Total Reaction Cross Section for Heavy-Ion Collisions and Its Relation to the Neutron Excess Degree of Freedom. *Nucl. Phys.*, vol. A491, 1989, pp. 130–146.
12. Vitturi, A.; and Zardi, F.: Modified Glauber Model for the Description of Elastic Scattering Between Heavy Ions. *Phys. Rev. C*, vol. 36, no. 4, Oct. 1987, pp. 1404–1407.
13. Sihver, L.; Tsao, C. H.; Silberberg, R.; Kanai, T.; and Barghouty, A. F.: Total Reaction and Partial Cross Section Calculations in Proton-Nucleus ($Z_t \leq 26$) and Nucleus-Nucleus Reactions (Z_p and $Z_t \leq 26$). *Phys. Rev. C*, vol. 47, no. 3, Mar. 1993, pp. 1225–1236.
14. DeVries, R. M.; and Peng, J. C.: Nucleus-Nucleus Total Reaction Cross Sections. *Phys. Rev. C*, vol. 22, no. 3, Sept. 1980, pp. 1055–1064.
15. Bauhoff, W.: Tables of Reaction and Total Cross Sections for Proton-Nucleus Scattering Below 1 GeV. *At. Data & Nucl. Data Tables*, vol. 35, 1986, pp. 429–447.
16. Kox, S.; Gamp, A.; Perrin, C.; Arvieux, J.; Bertholet, R.; Bruandet, J. F.; Buenerd, M.; Cherkaoui, R.; Cole, A. J.; El-Masri, Y.; Longequeue, N.; Menet, J.; Merchex, F.; and Viano, J. B.: Trends of Total Reaction Cross Sections for Heavy Ion Collisions in the Intermediate Energy Range. *Phys. Rev. C*, vol. 35, no. 5, May 1987, pp. 1678–1691.
17. Barashenkov, V. S.; Gudima, K. K.; and Toneev, V. D.: Cross Sections for Fast Particles and Atomic Nuclei. *Prog. Phys.*, vol. 17, no. 10, 1969, pp. 683–725.
18. Webber, W. R.; Kish, J. C.; and Schrier, D. A.: Formula for Calculating Partial Cross Sections for Nuclear Reactions of Nuclei With $E \geq 200$ MeV/Nucleon in Hydrogen Targets. *Phys. Rev. C*, vol. 41, no. 2, Feb. 1990, pp. 566–571.
19. Dubar, L. V.; Eleukenov, D. Sh.; Slyusarenko, L. I.; and Yurkuts, N. P.: Parametrization of Total Cross Sections of Reactions in the Intermediate Energy Region. *Sov. J. Nucl. Phys.*, vol. 49, no. 5, May 1989, pp. 771–773.
20. Menet, J. J. H.; Gross, E. E.; Malanify, J. J.; and Zucker, A.: Total-Reaction-Cross-Section Measurements for 30-60 MeV Protons and the Imaginary Optical Potential. *Phys. Rev. C*, no. 4, Oct. 1971, pp. 1114–1129.
21. Riisager, K.: Nuclear Halo States. *Rev. Mod. Phys.*, vol. 66, no. 3, July 1994, pp. 1105–1116.
22. Auce, A.; Carlson, R. F.; Cox, A. J.; Ingemarsson, A.; Johansson, R.; Renberg, P. U.; Sundberg, O.; and Tibell, G.: Reaction Cross Sections for 75–190 MeV Alpha Particles on Targets From ^{12}C to ^{208}Pb . *Phys. Rev. C*, vol. 50, no. 2, Aug. 1994, pp. 871–879.
23. Jaros, J.; Wagner, A.; Anderson, L.; Chamberlain, O.; Fuzesy, R. Z.; Gallup, J.; Gorn, W.; Schroeder, L.; Shannon, S.; Shapiro, G.; and Steiner, H.: Nucleus-Nucleus Total Cross Sections for Light Nuclei at 1.55 and 2.89 GeV/c Per Nucleon. *Phys. Rev. C*, vol. 18, 1978, pp. 2273–2292.
24. Heckman, H. H.; Greiner, D. E.; Lindstrom, P. J.; and Shwe, H.: Fragmentation of ^4He , ^{12}C , ^{14}N , and ^{16}O Nuclei in Nuclear Emulsion at 2.1 GeV/Nucleon. *Phys. Rev. C*, vol. 17, no. 5, May 1978, pp. 1735–1747.

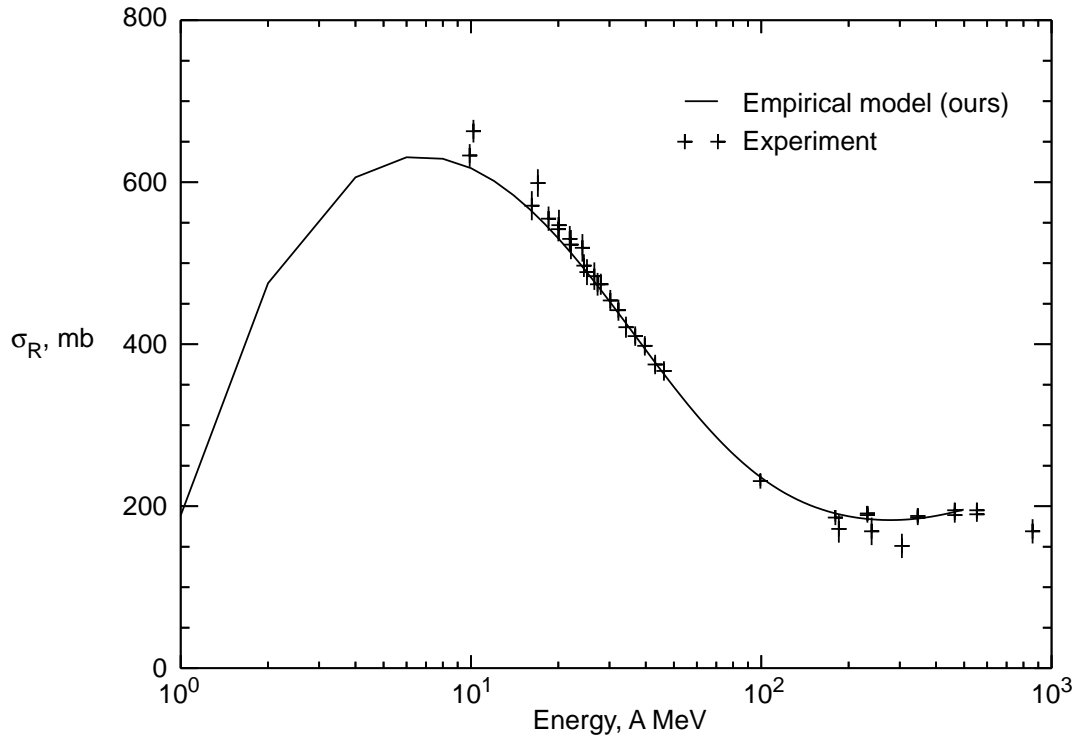


Figure 1. Reaction cross sections as a function of energy for $p + {}^9_4\text{Be}$ collisions.

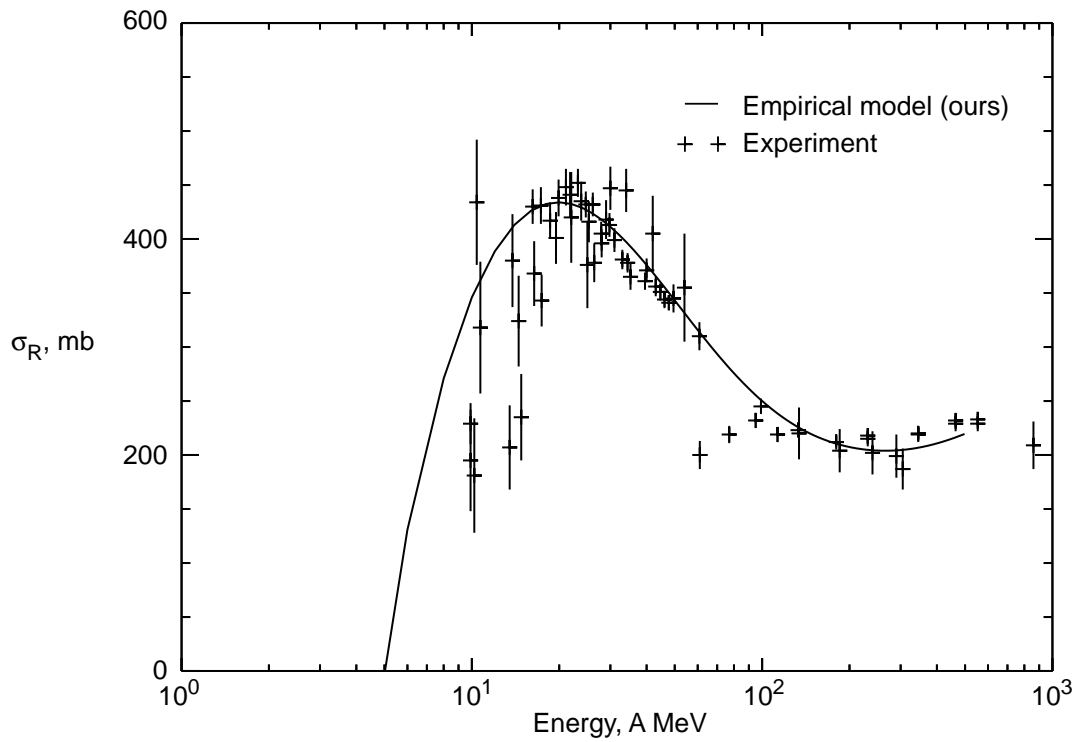


Figure 2. Reaction cross sections as a function of energy for $p + {}^{12}_6\text{C}$ collisions.

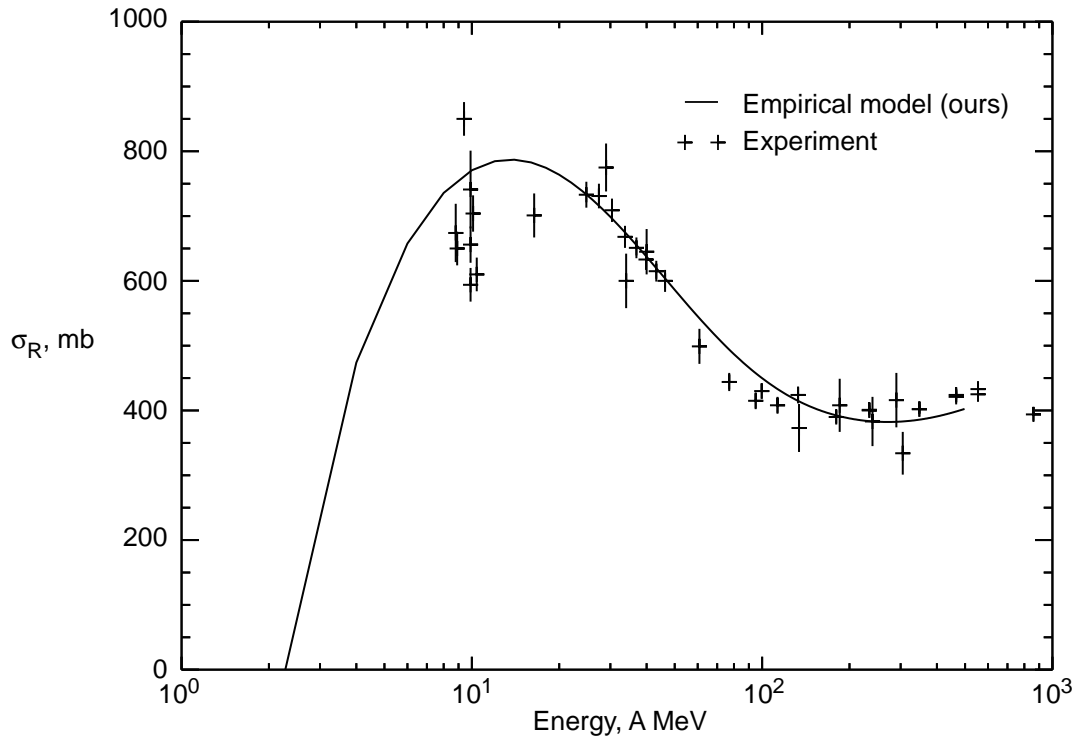


Figure 3. Reaction cross sections as a function of energy for $p + {}^{27}_{13}\text{Al}$ collisions.

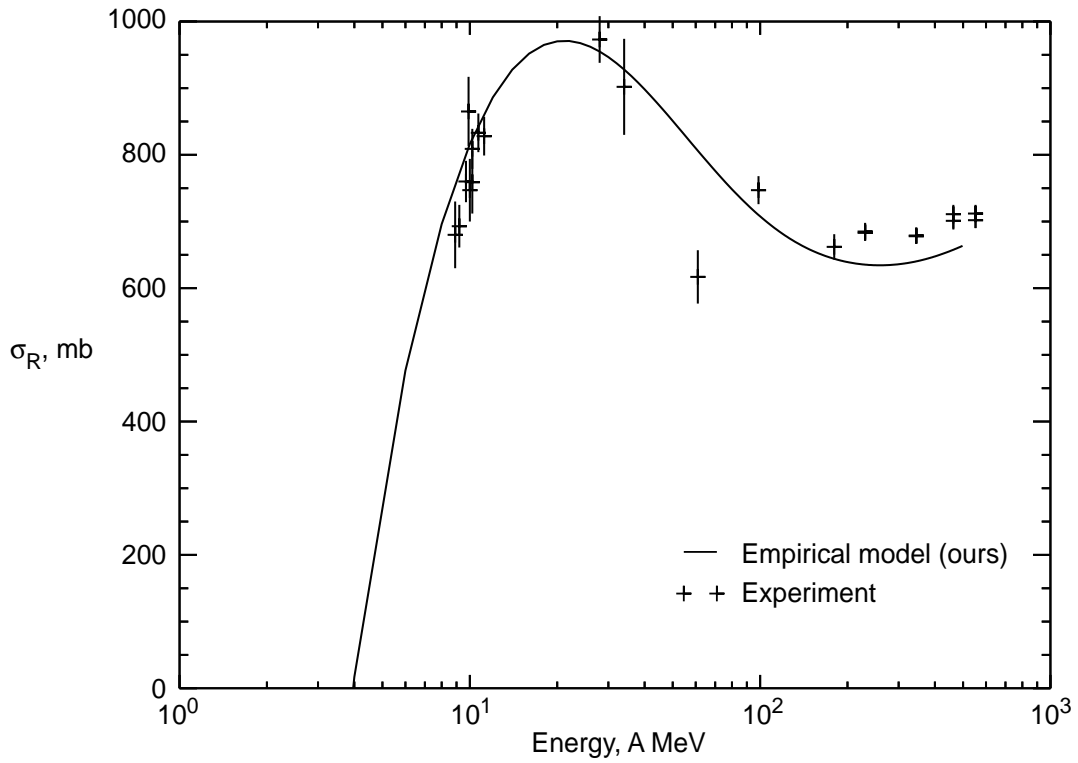


Figure 4. Reaction cross sections as a function of energy for $p + {}^{\text{nat}}_{26}\text{Fe}$ collisions.

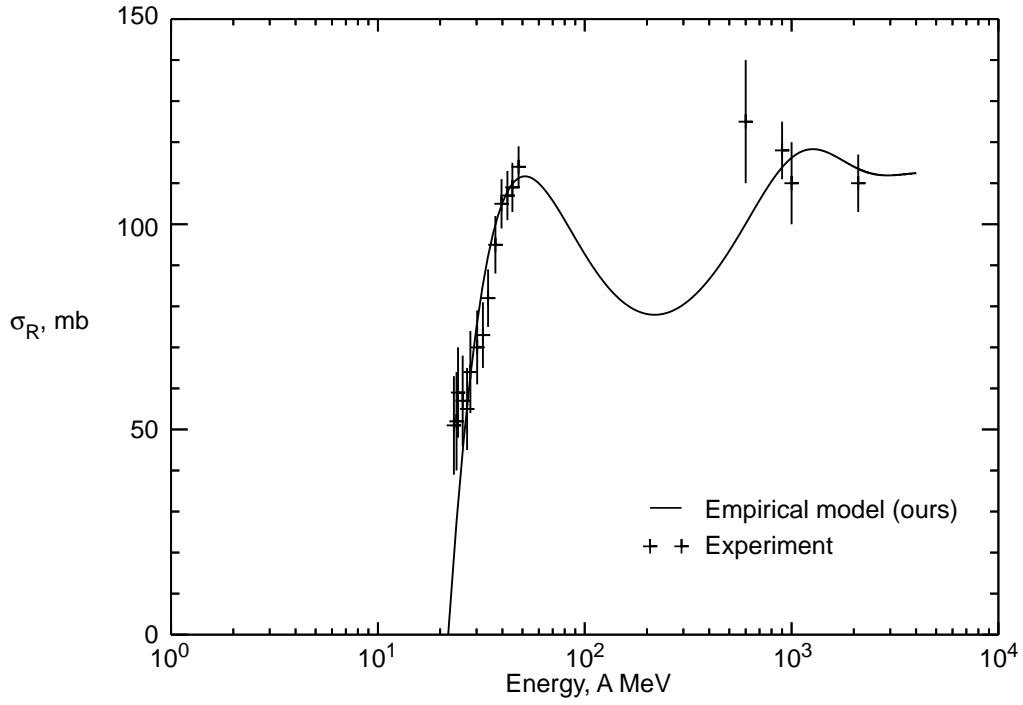


Figure 5. Reaction cross sections as a function of energy for $\alpha + {}^1_1\text{H}$ collisions.

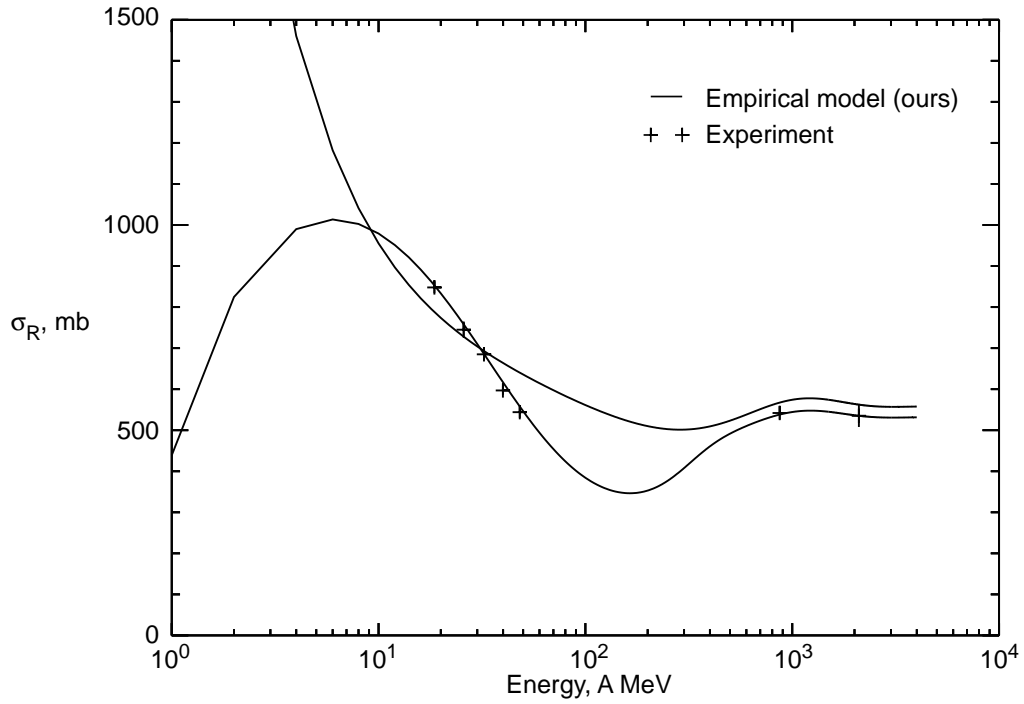


Figure 6. Reaction cross sections as a function of energy for $\alpha + {}^{12}_6\text{C}$ collisions; dashed line is from reference 10.

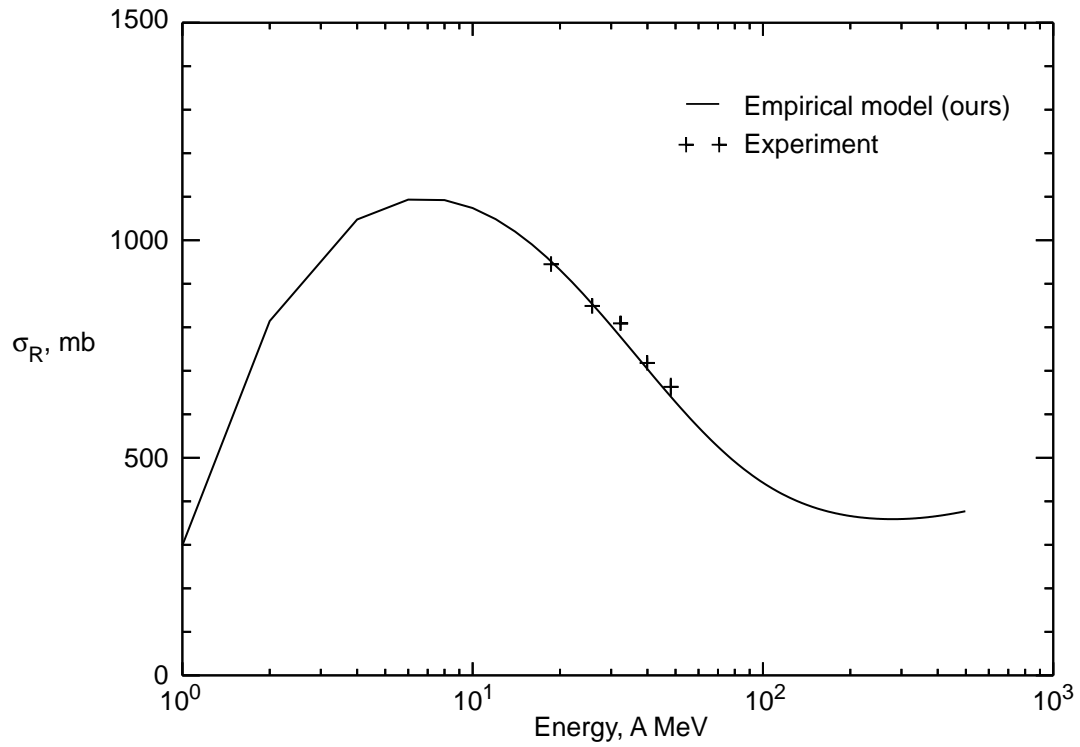


Figure 7. Reaction cross sections as a function of energy for $\alpha + {}^{16}_8\text{O}$ collisions.

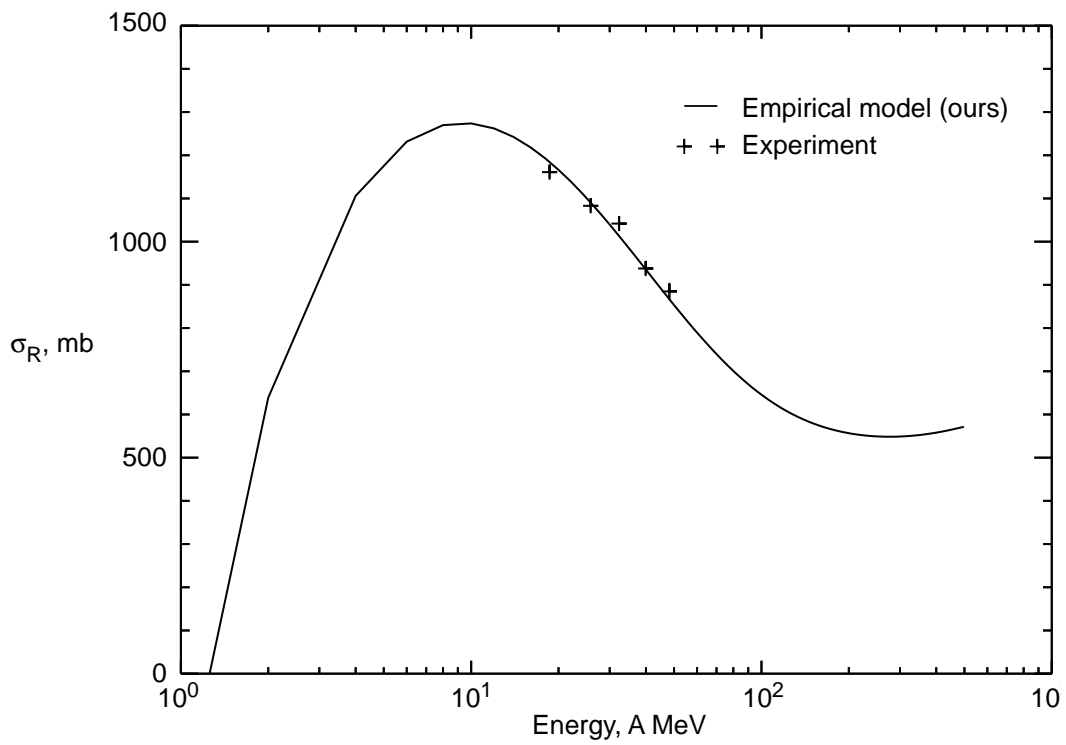


Figure 8. Reaction cross sections as a function of energy for $\alpha + {}^{28}_{14}\text{Si}$ collisions.

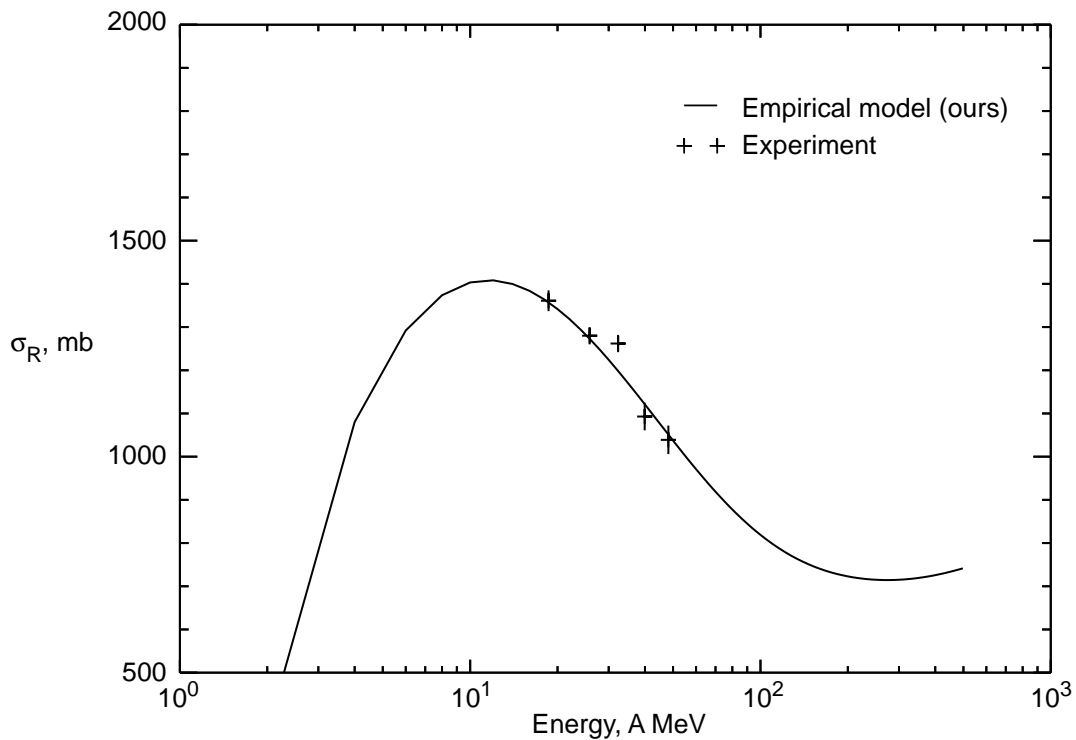


Figure 9. Reaction cross sections as a function of energy for $\alpha + {}^{40}\text{Ca}$ collisions.

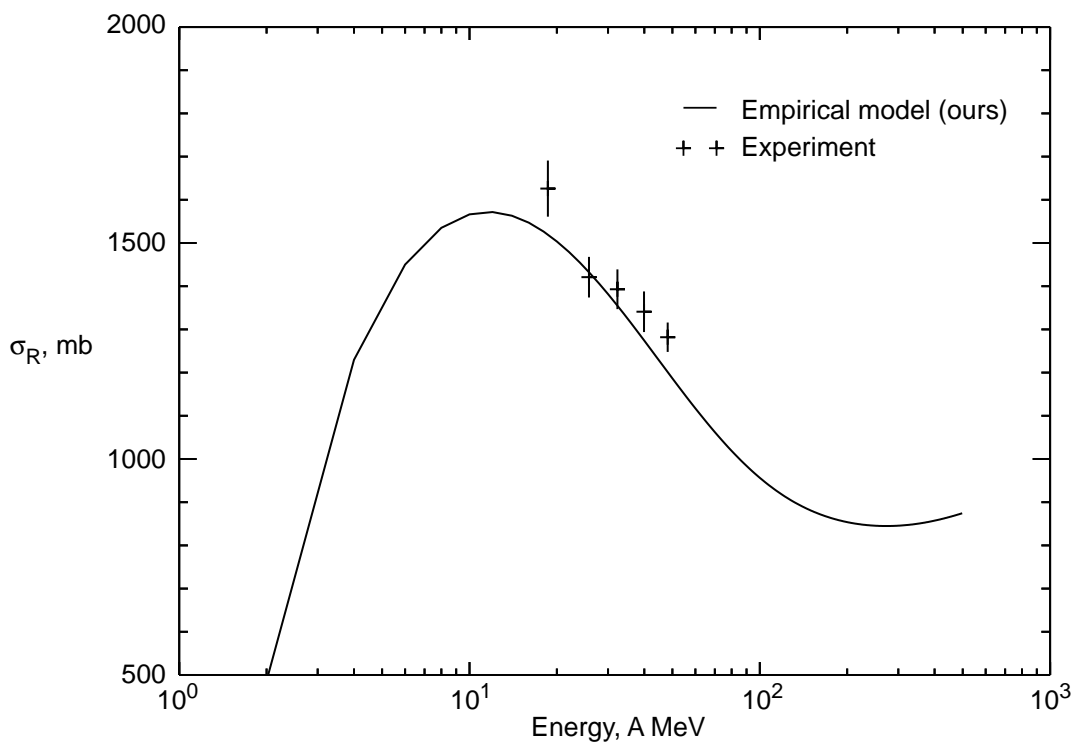


Figure 10. Reaction cross sections as a function of energy for $\alpha + {}^{48}\text{Ca}$ collisions.

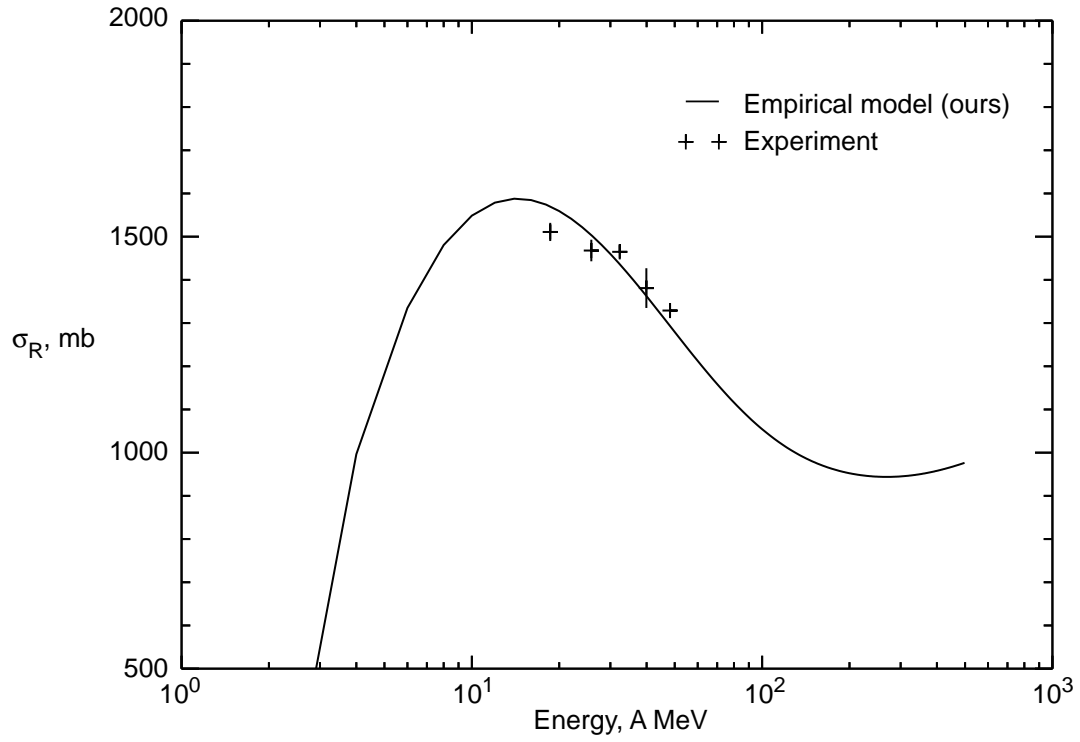


Figure 11. Reaction cross sections as a function of energy for $\alpha + {}^{58}\text{Ni}$ collisions.

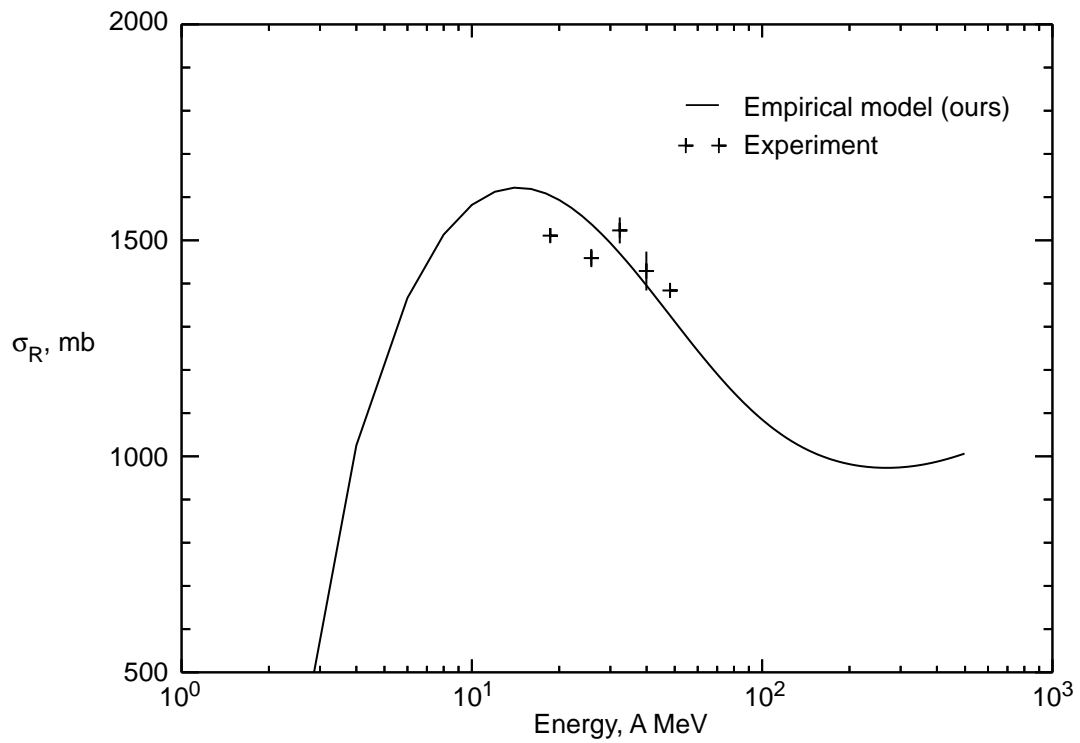


Figure 12. Reaction cross sections as a function of energy for $\alpha + {}^{60}\text{Ni}$ collisions.

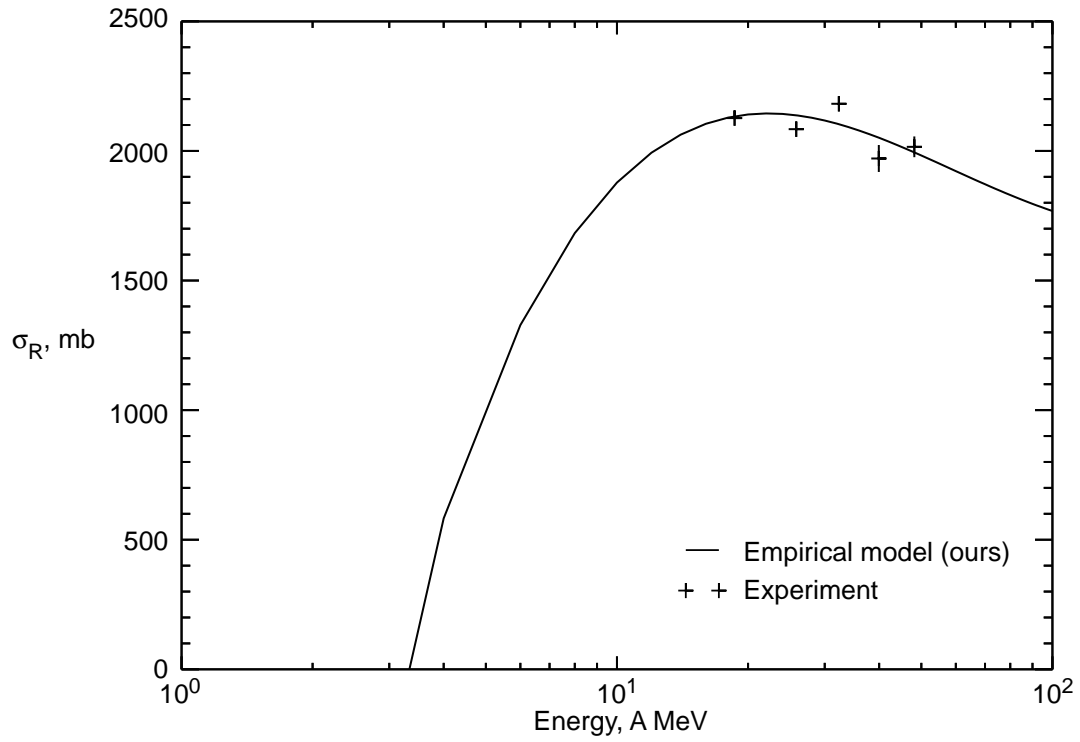


Figure 13. Reaction cross sections as a function of energy for $\alpha + {}^{124}_{50}\text{Sn}$ collisions.

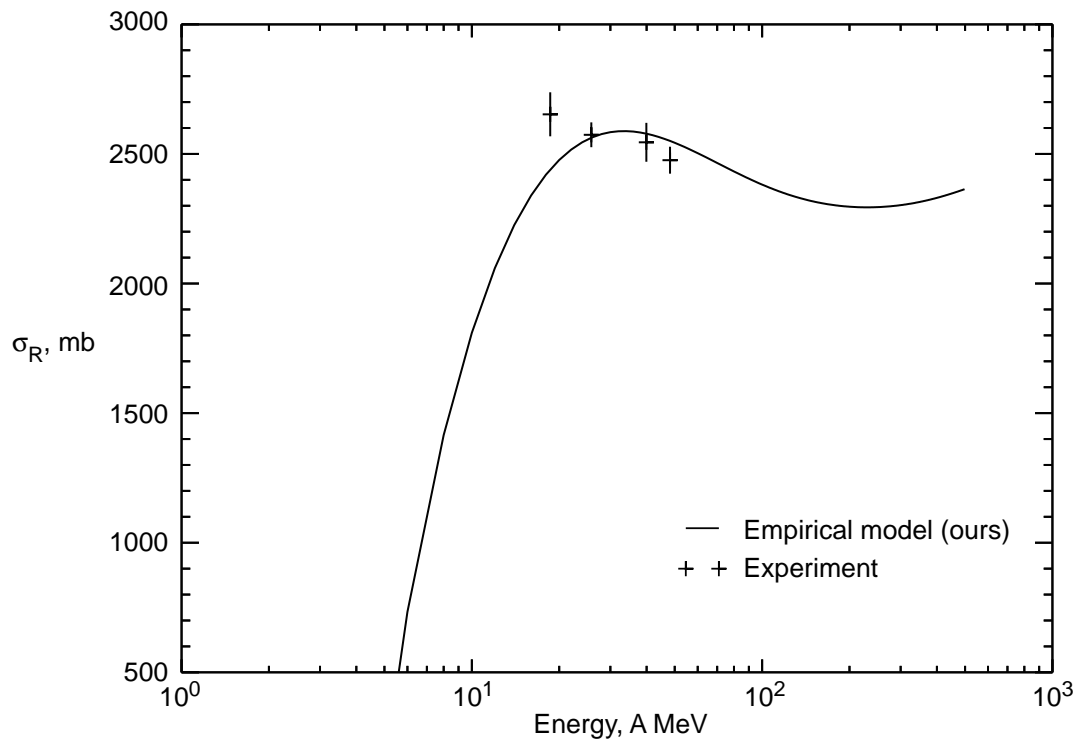


Figure 14. Reaction cross sections as a function of energy for $\alpha + {}^{208}_{82}\text{Pb}$ collisions.

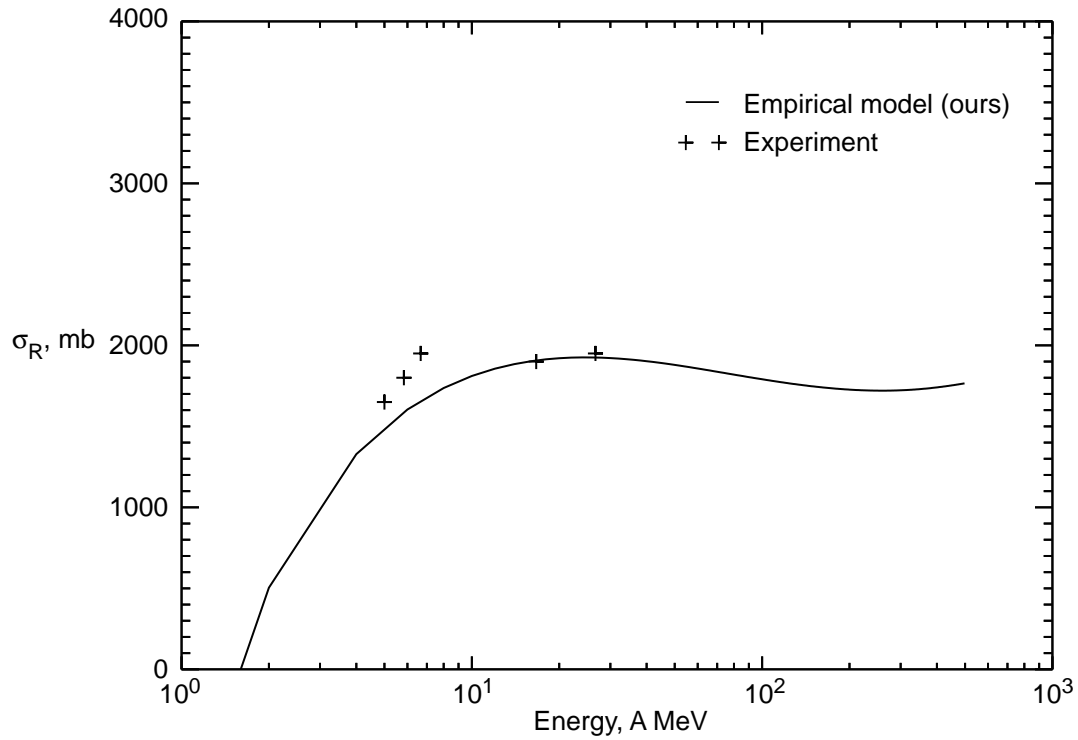


Figure 15. Reaction cross sections as a function of energy for ${}^6_3\text{Li} + {}^{40}_{20}\text{Ca}$ collisions.

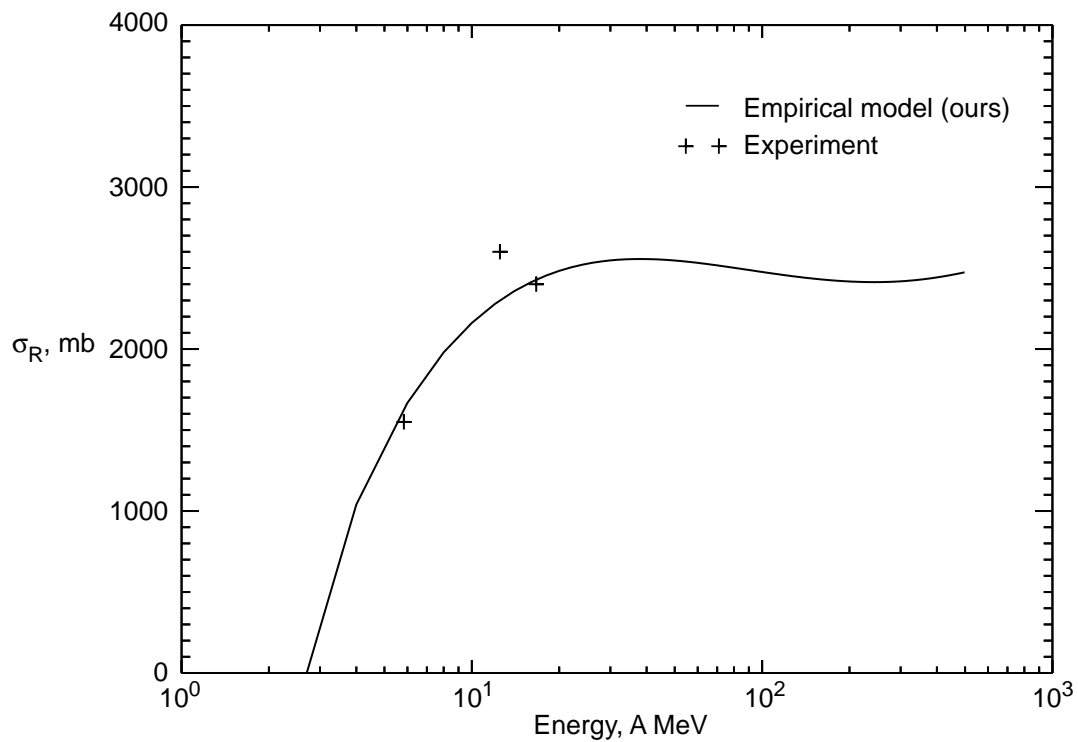


Figure 16. Reaction cross sections as a function of energy for ${}^6_3\text{Li} + {}^{90}_{40}\text{Zr}$ collisions.

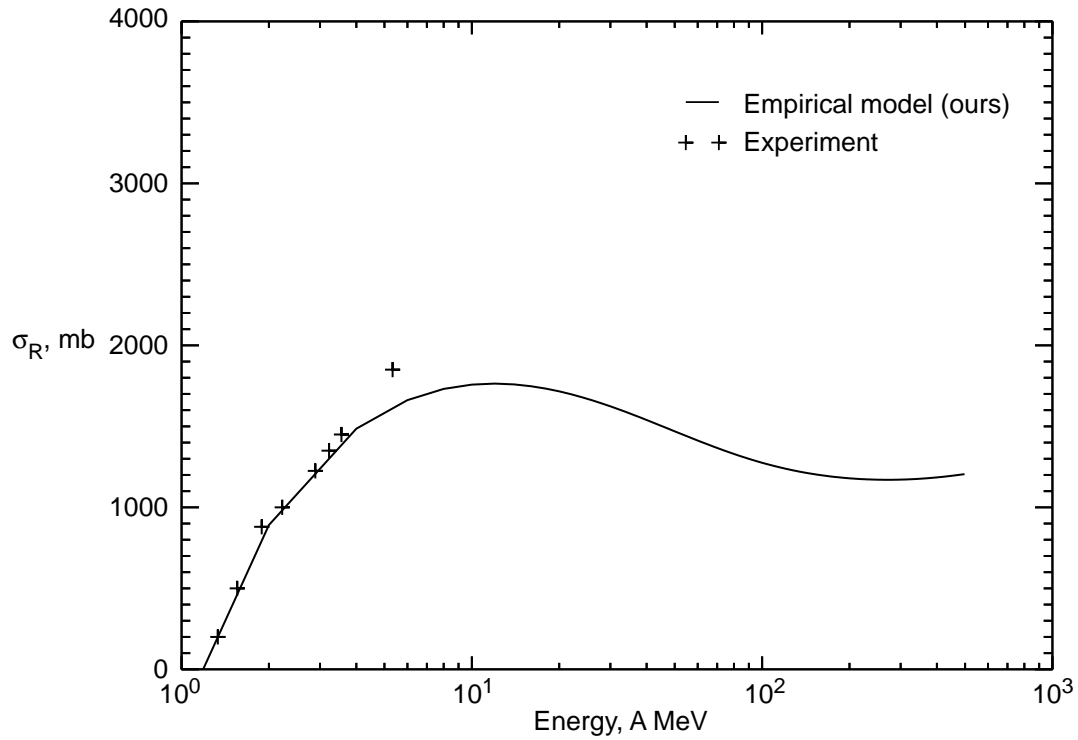


Figure 17. Reaction cross sections as a function of energy for ${}^9_4\text{Be} + {}^{28}_{14}\text{Si}$ collisions.

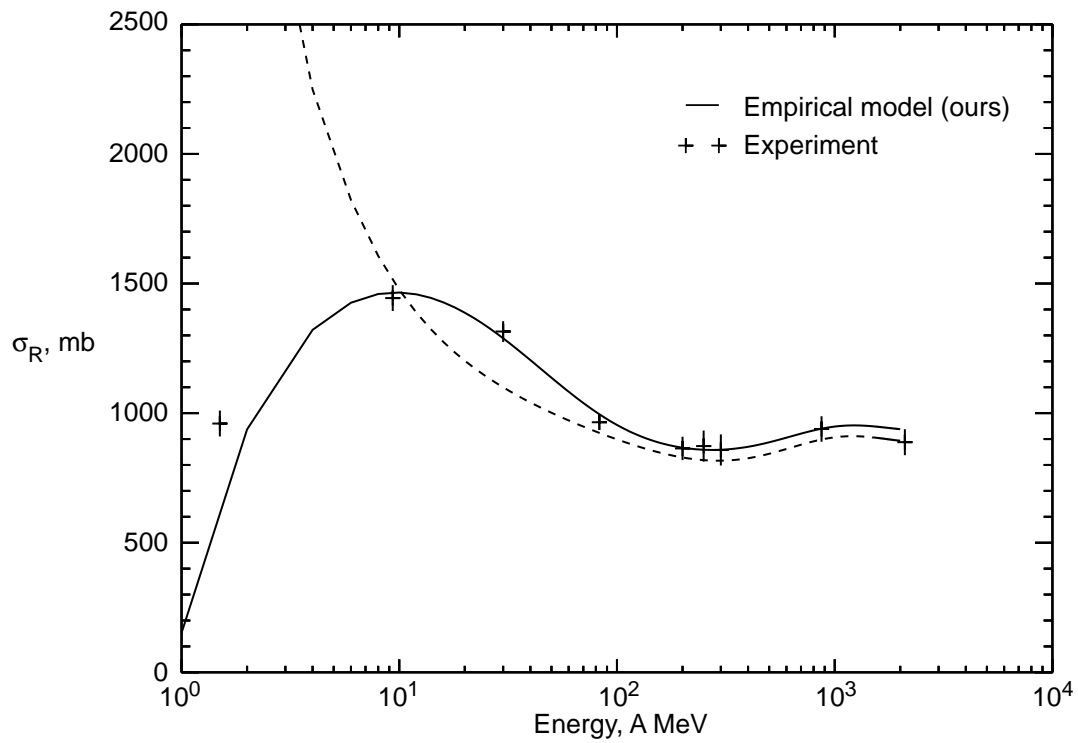


Figure 18. Reaction cross sections as a function of energy for ${}^{12}_6\text{C} + {}^{12}_6\text{C}$ collisions; dashed line is from reference 18.

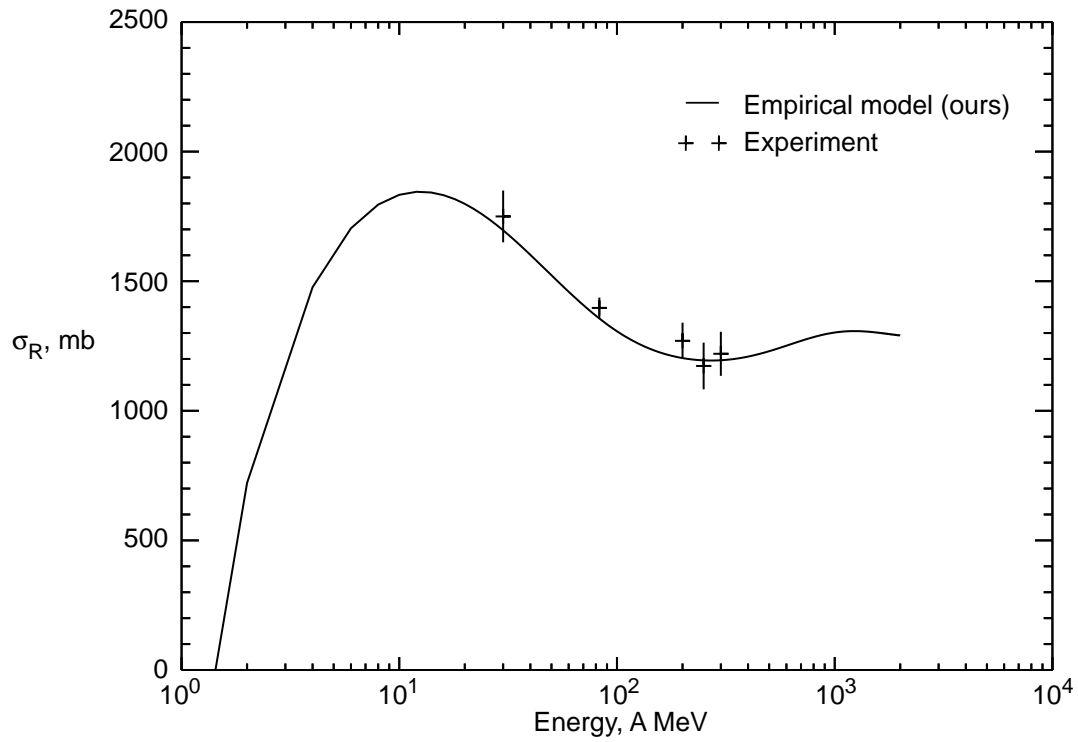


Figure 19. Reaction cross sections as a function of energy for $^{12}_6\text{C} + ^{27}_{13}\text{Al}$ collisions.

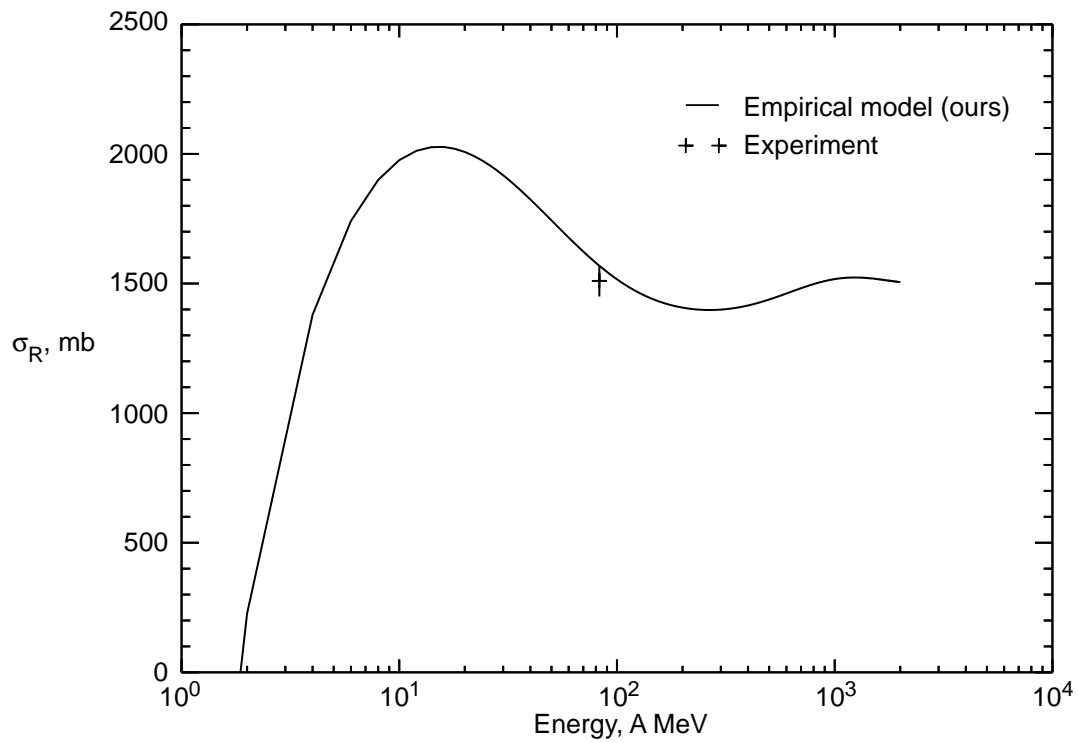


Figure 20. Reaction cross sections as a function of energy for $^{12}_6\text{C} + ^{40}_{20}\text{Ca}$ collisions.

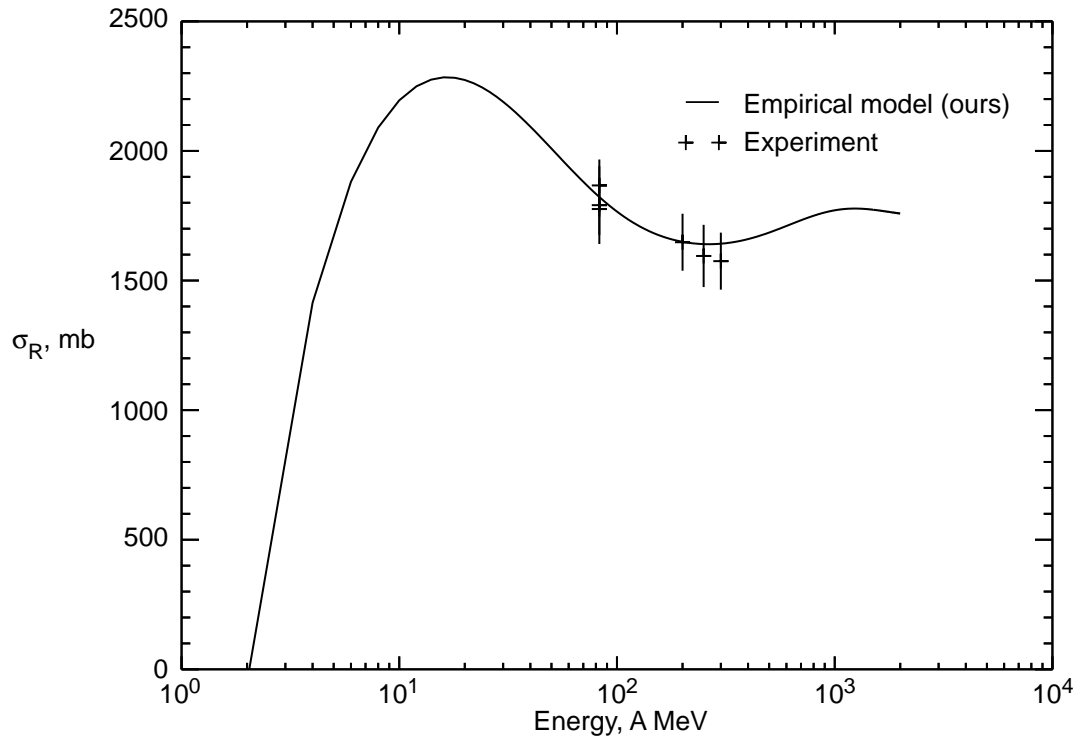


Figure 21. Reaction cross sections as a function of energy for $^{12}_6\text{C} + ^{56}_{26}\text{Fe}$ collisions.

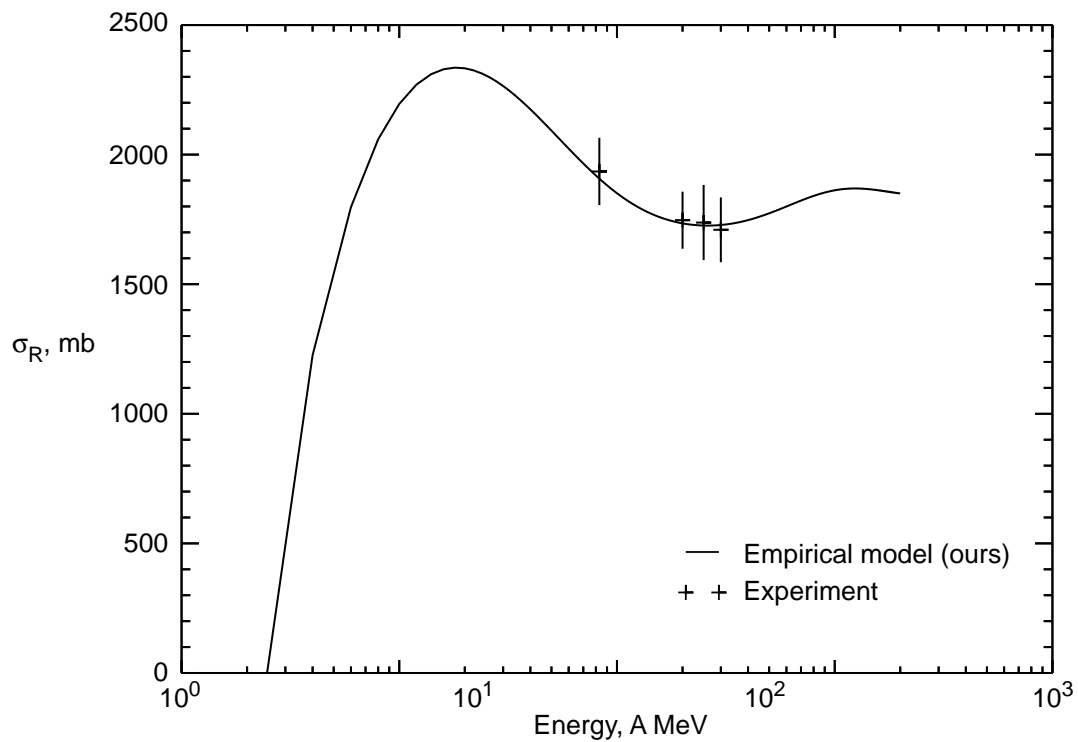


Figure 22. Reaction cross sections as a function of energy for $^{12}_6\text{C} + ^{64}_{30}\text{Zn}$ collisions.

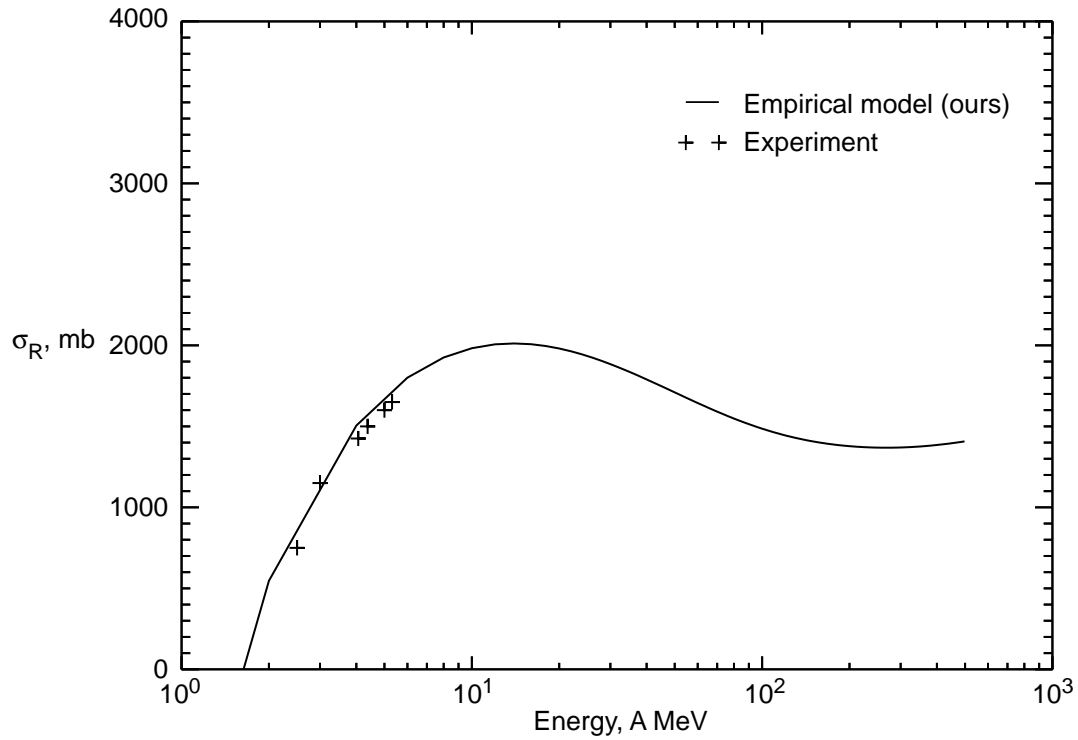


Figure 23. Reaction cross sections as a function of energy for $^{16}\text{O} + ^{28}\text{Si}$ collisions.

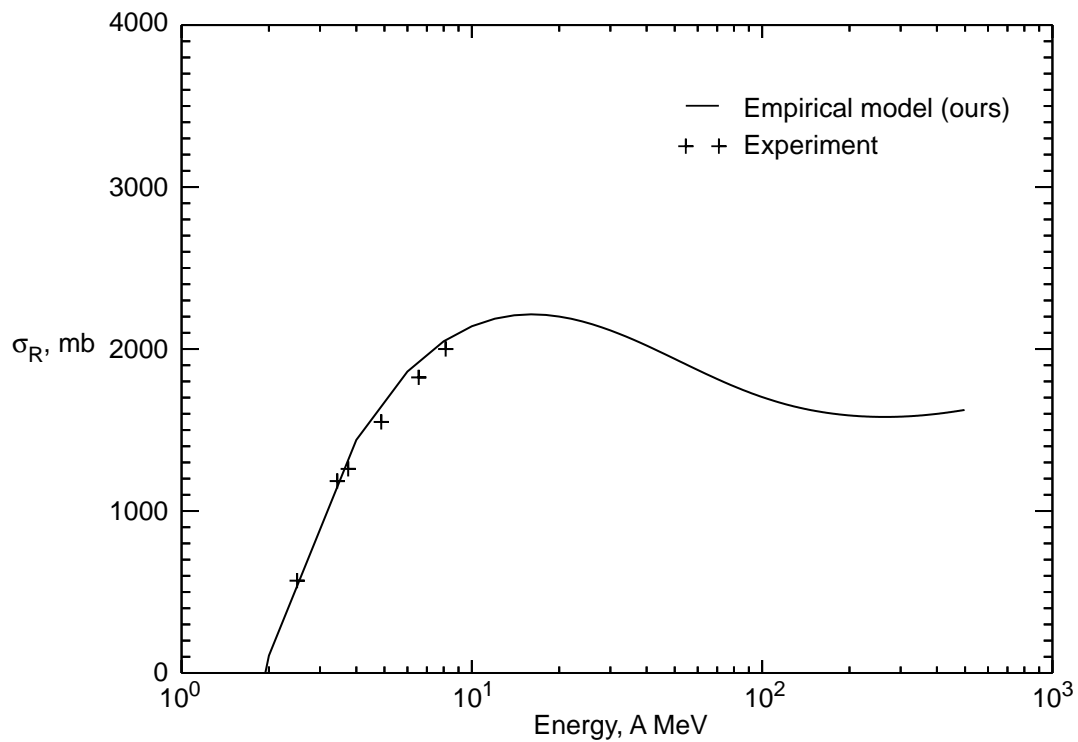


Figure 24. Reaction cross sections as a function of energy for $^{16}\text{O} + ^{40}\text{Ca}$ collisions.

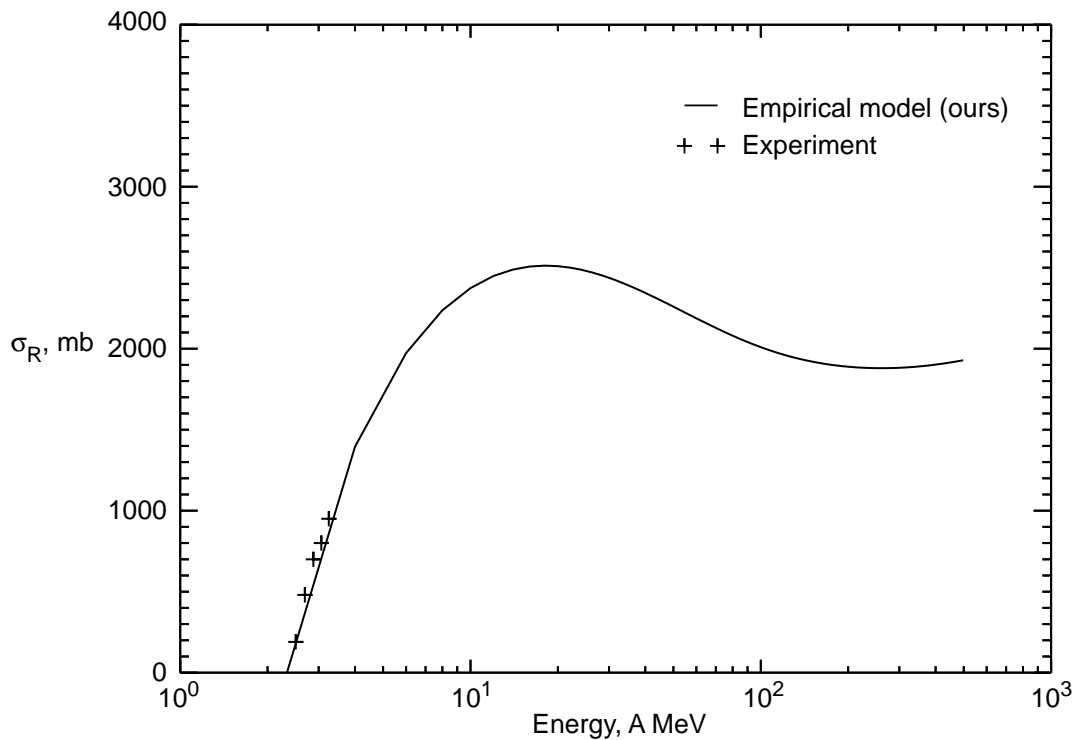


Figure 25. Reaction cross sections as a function of energy for $^{16}\text{O} + ^{59}\text{Co}$ collisions.

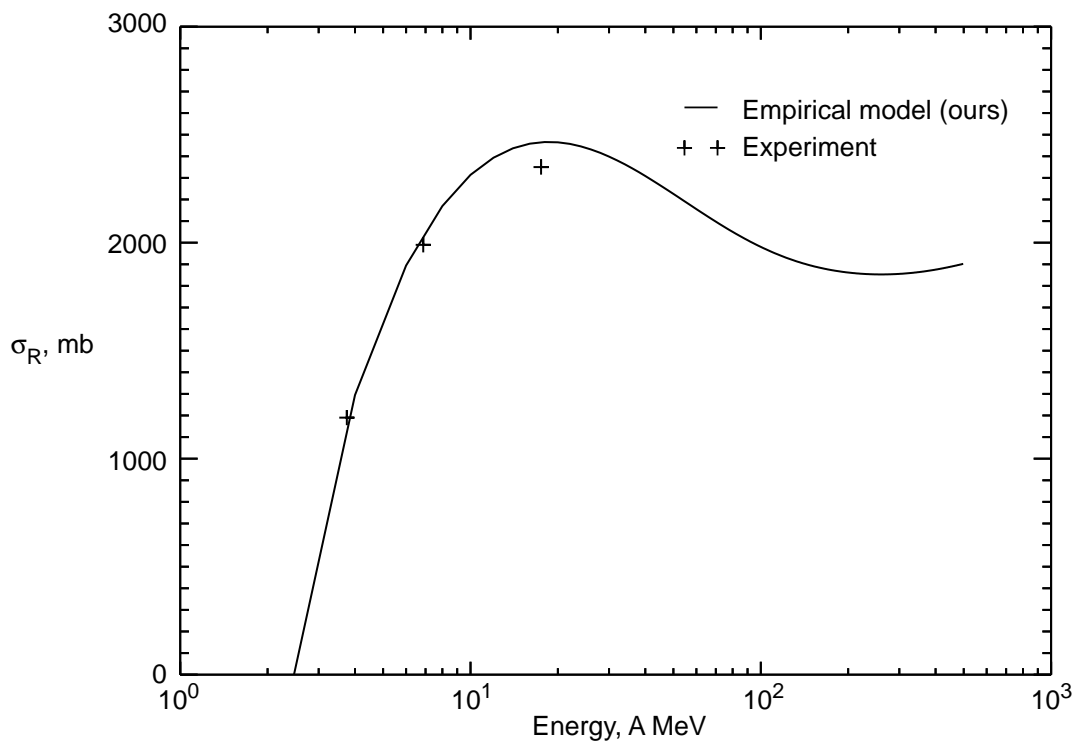


Figure 26. Reaction cross sections as a function of energy for $^{16}\text{O} + ^{58}\text{Ni}$ collisions.

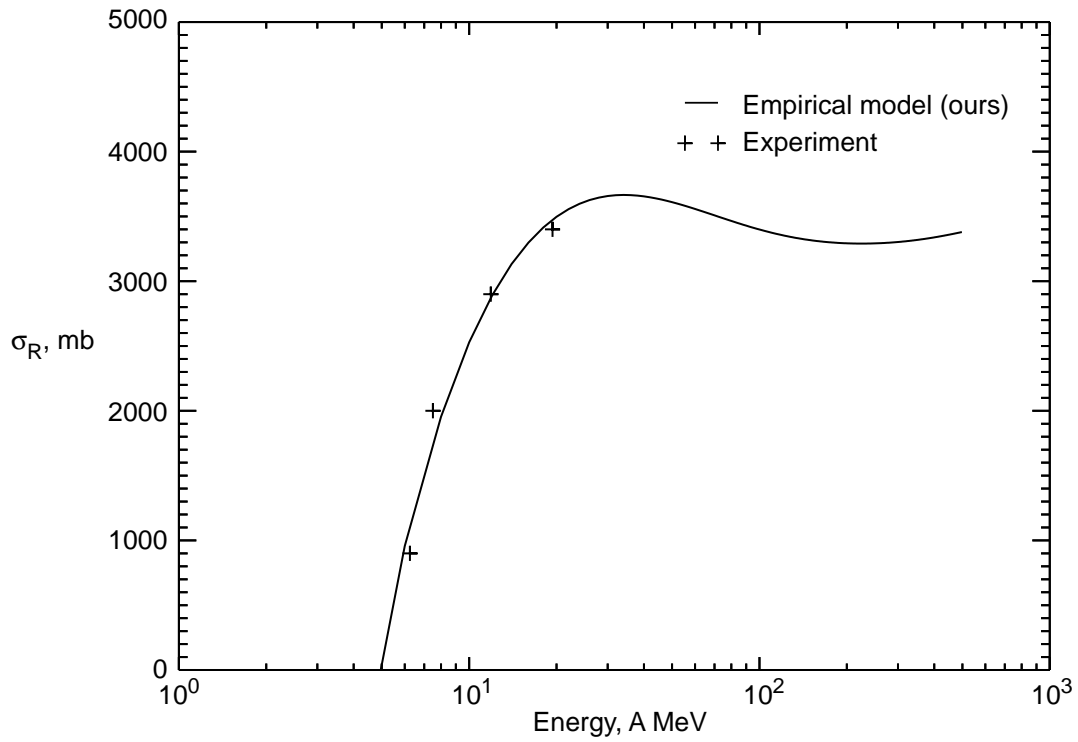


Figure 27. Reaction cross sections as a function of energy for $^{16}_8\text{O} + ^{208}_{82}\text{Pb}$ collisions.

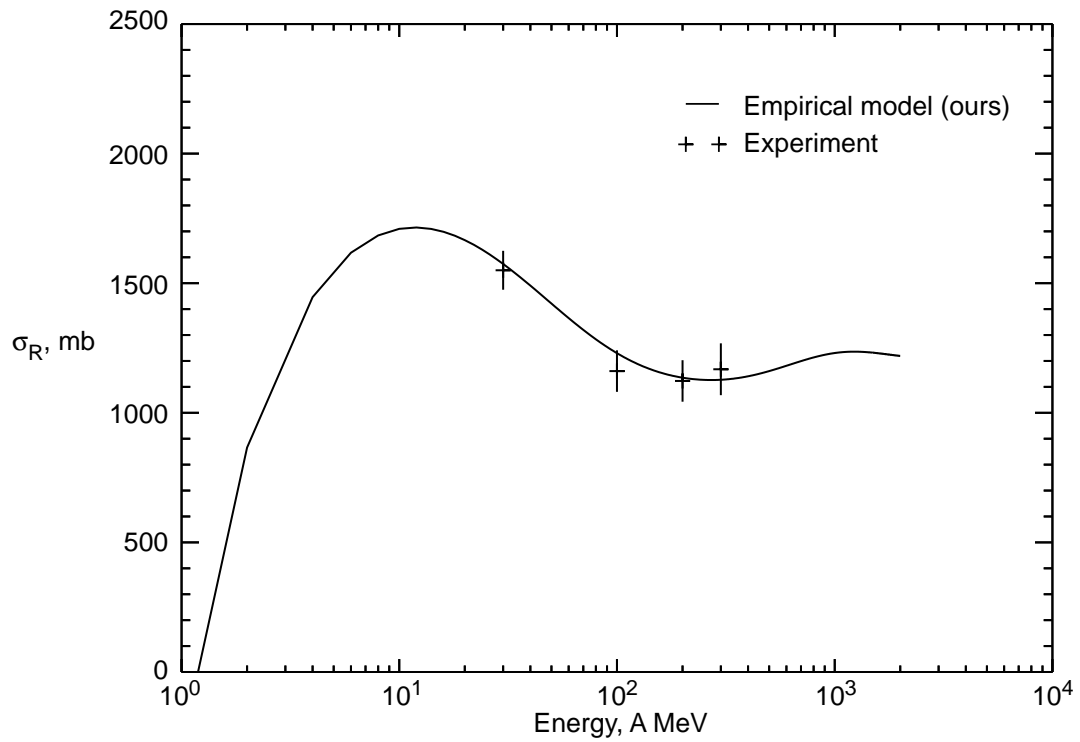


Figure 28. Reaction cross sections as a function of energy for $^{20}_{10}\text{Ne} + ^{12}_6\text{C}$ collisions.

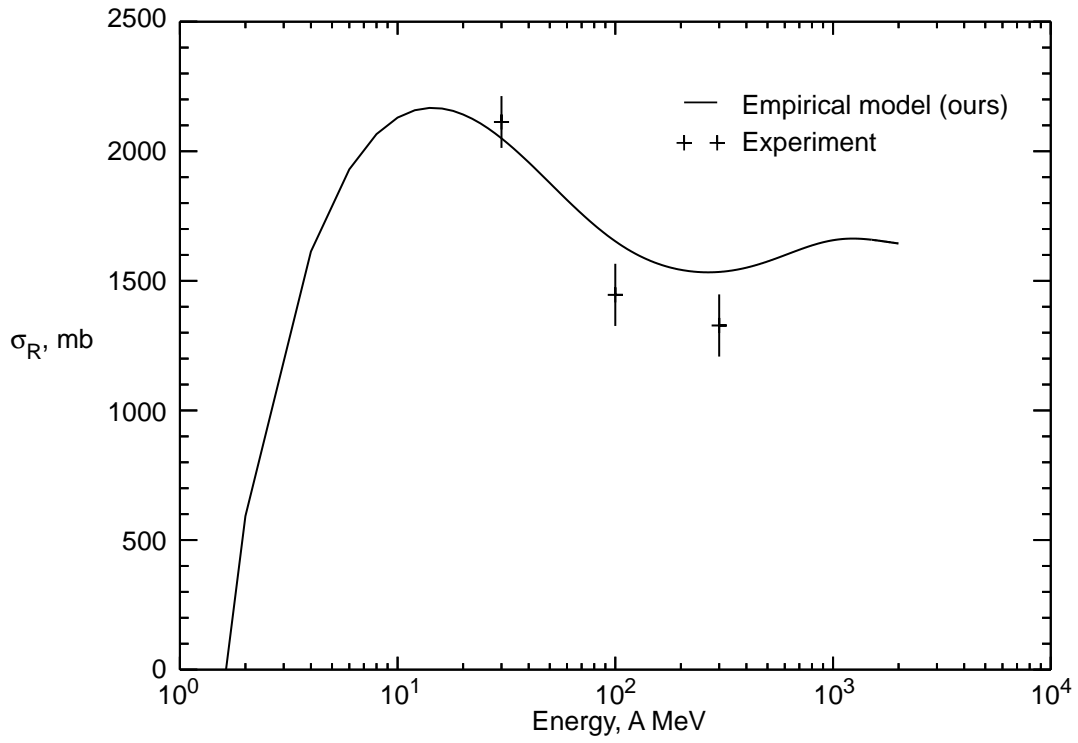


Figure 29. Reaction cross sections as a function of energy for $^{20}_{10}\text{Ne} + ^{27}_{13}\text{Al}$ collisions.

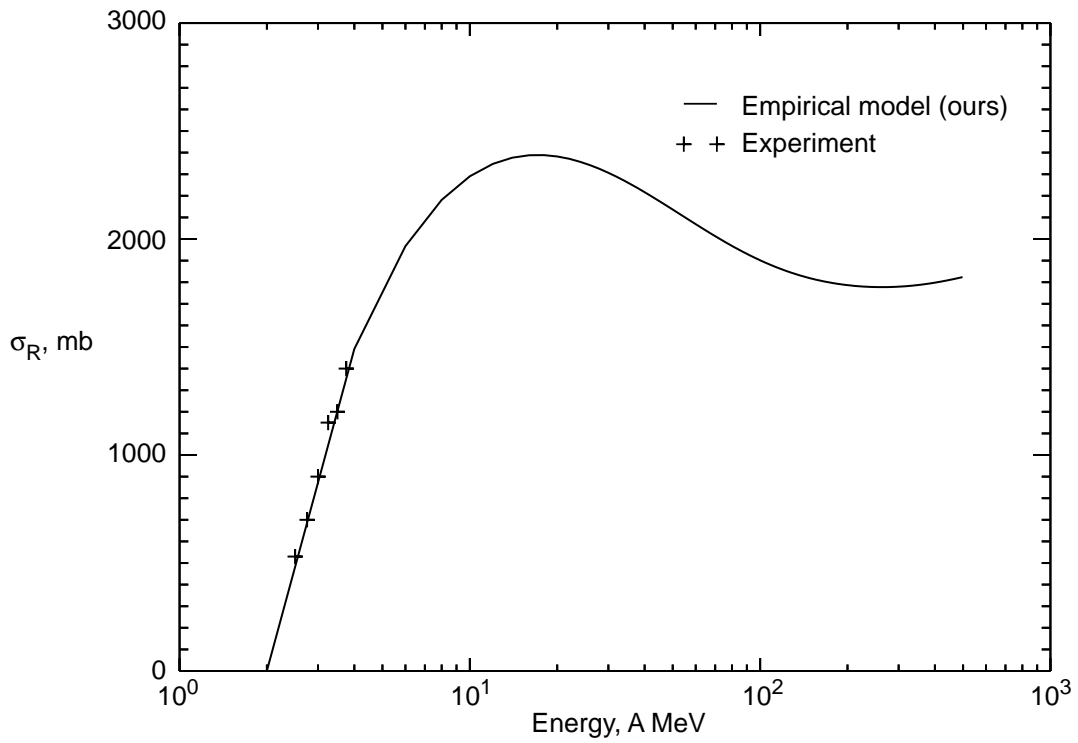


Figure 30. Reaction cross sections as a function of energy for $^{20}_{10}\text{Ne} + ^{40}_{20}\text{Ca}$ collisions.

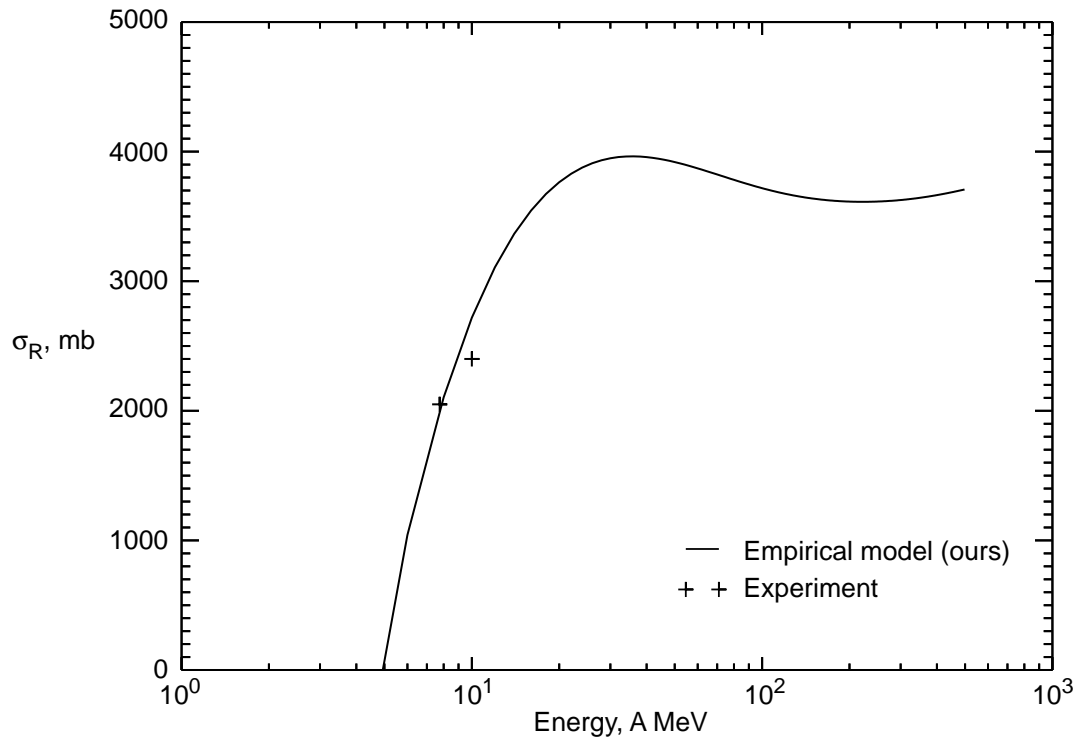


Figure 31. Reaction cross sections as a function of energy for $^{20}_{10}\text{Ne} + ^{208}_{82}\text{Pb}$ collisions.

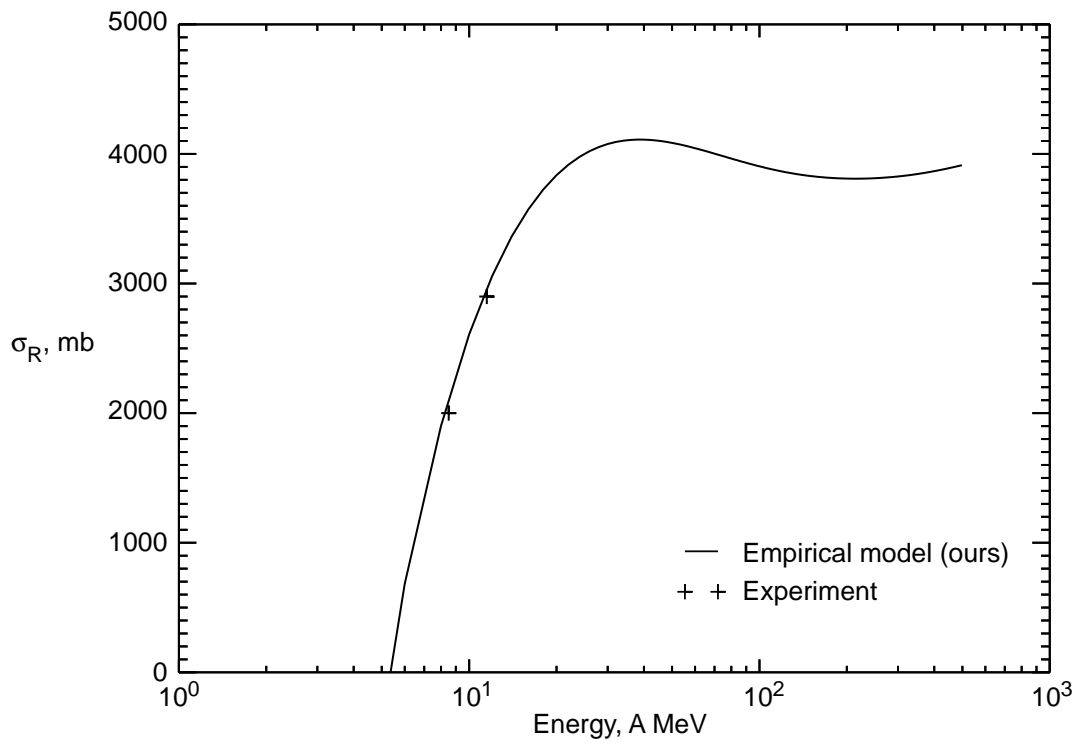


Figure 32. Reaction cross sections as a function of energy for $^{20}_{10}\text{Ne} + ^{235}_{92}\text{U}$ collisions.

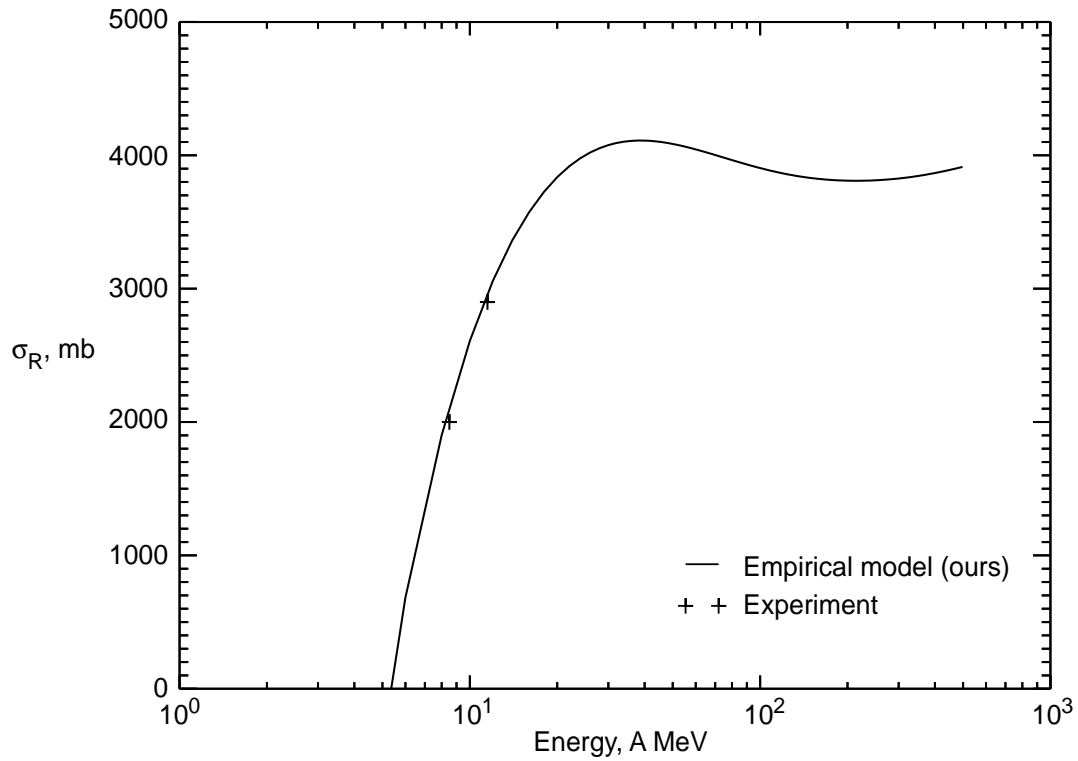


Figure 33. Reaction cross sections as a function of energy for $^{32}_{16}\text{S} + ^{24}_{12}\text{Mg}$ collisions.

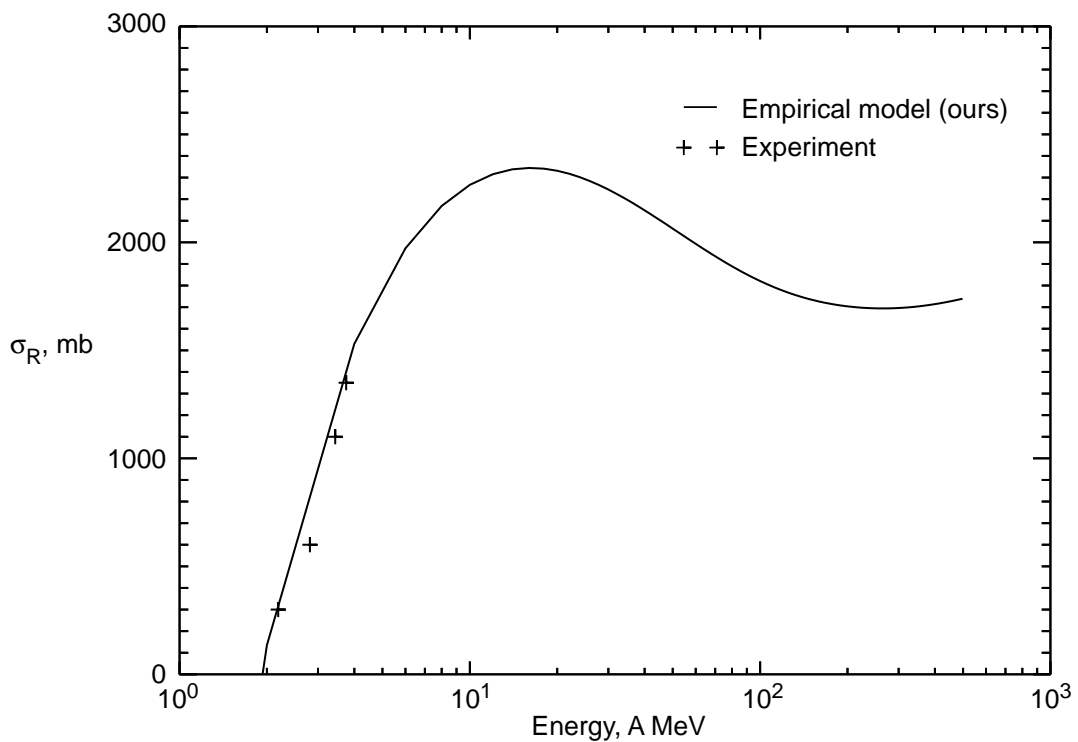


Figure 34. Reaction cross sections as a function of energy for $^{32}_{16}\text{S} + ^{27}_{13}\text{Al}$ collisions.

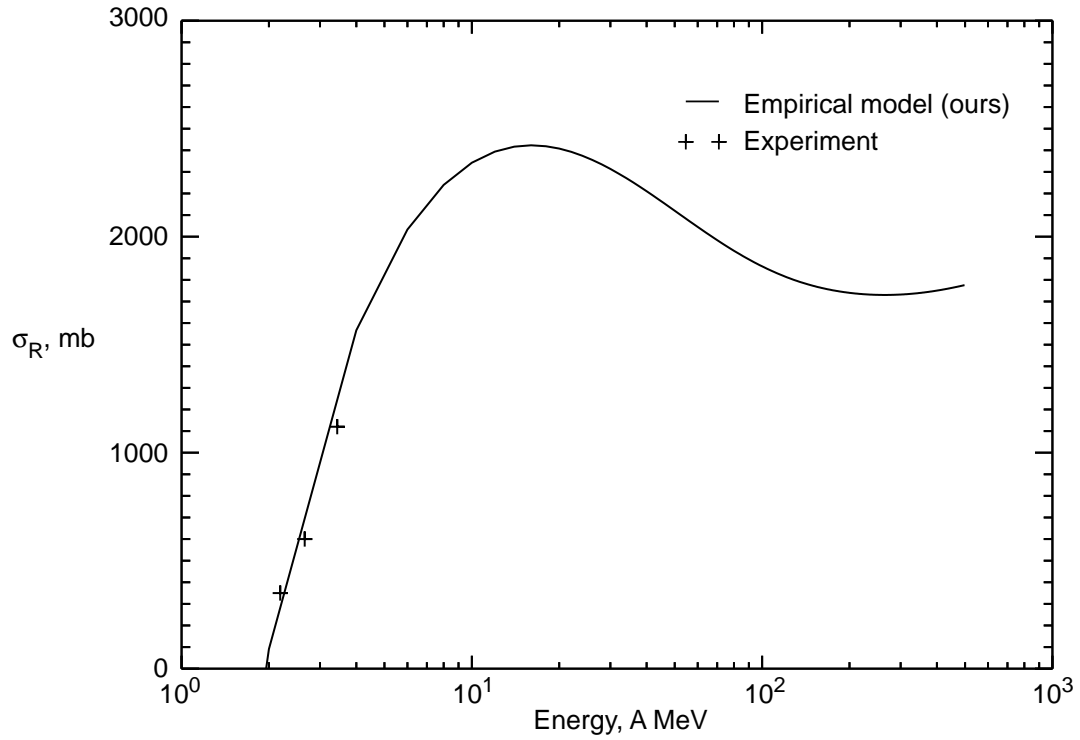


Figure 35. Reaction cross sections as a function of energy for $^{35}_{17}\text{Cl} + ^{58}_{28}\text{Ni}$ collisions.

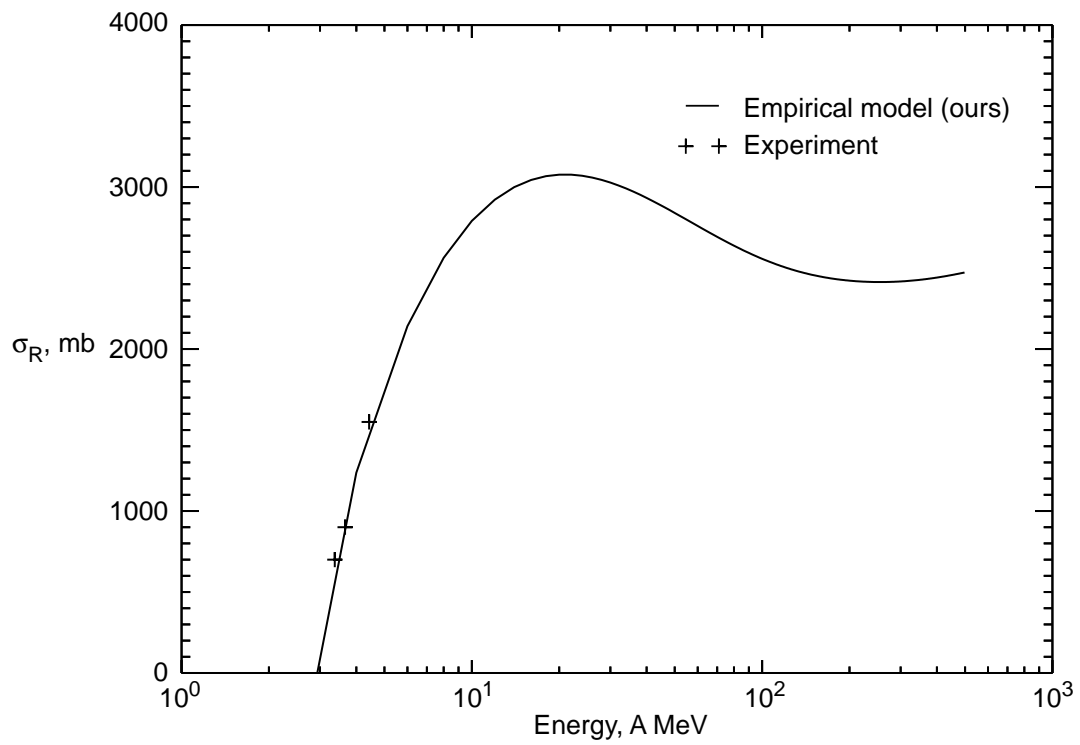


Figure 36. Reaction cross sections as a function of energy for $^{35}_{17}\text{Cl} + ^{62}_{28}\text{Ni}$ collisions.

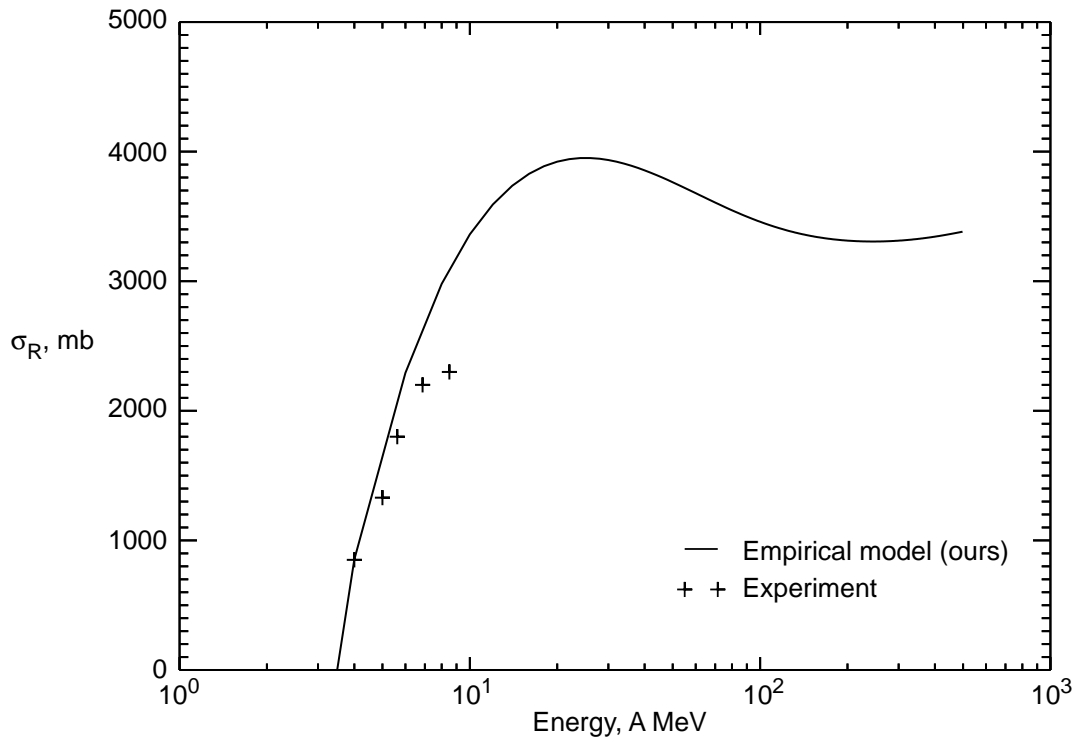


Figure 37. Reaction cross sections as a function of energy for $^{40}_{18}\text{Ar} + ^{109}_{47}\text{Ag}$ collisions.

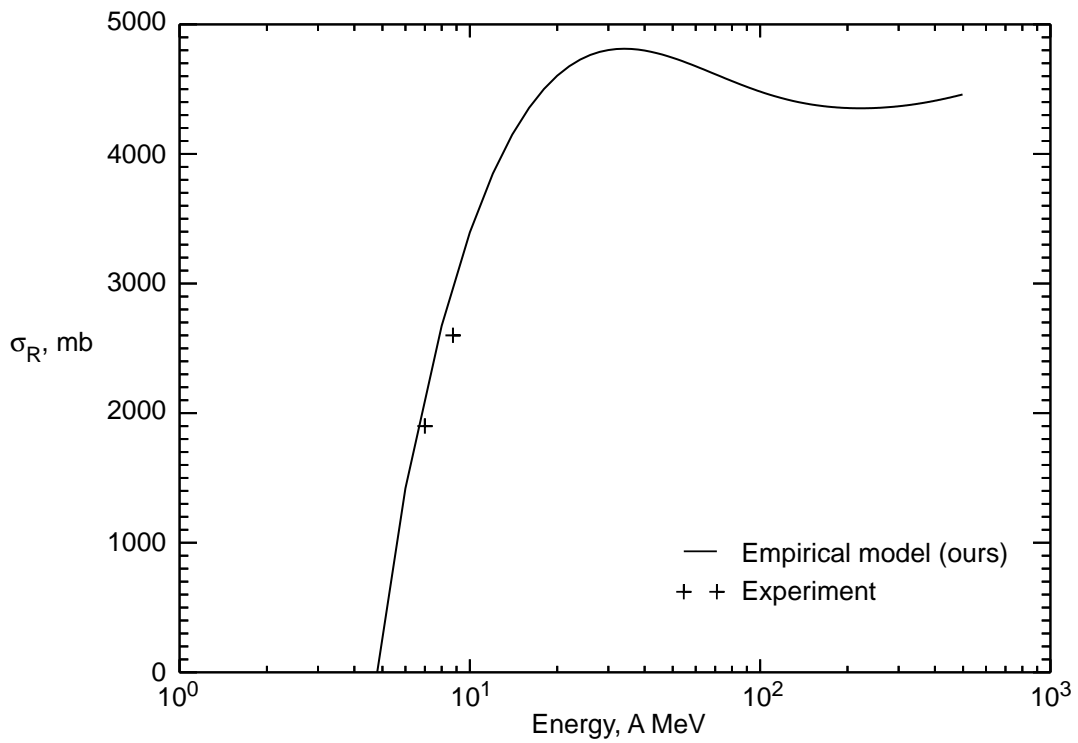


Figure 38. Reaction cross sections as a function of energy for $^{40}_{18}\text{Ar} + ^{209}_{83}\text{Bi}$ collisions.

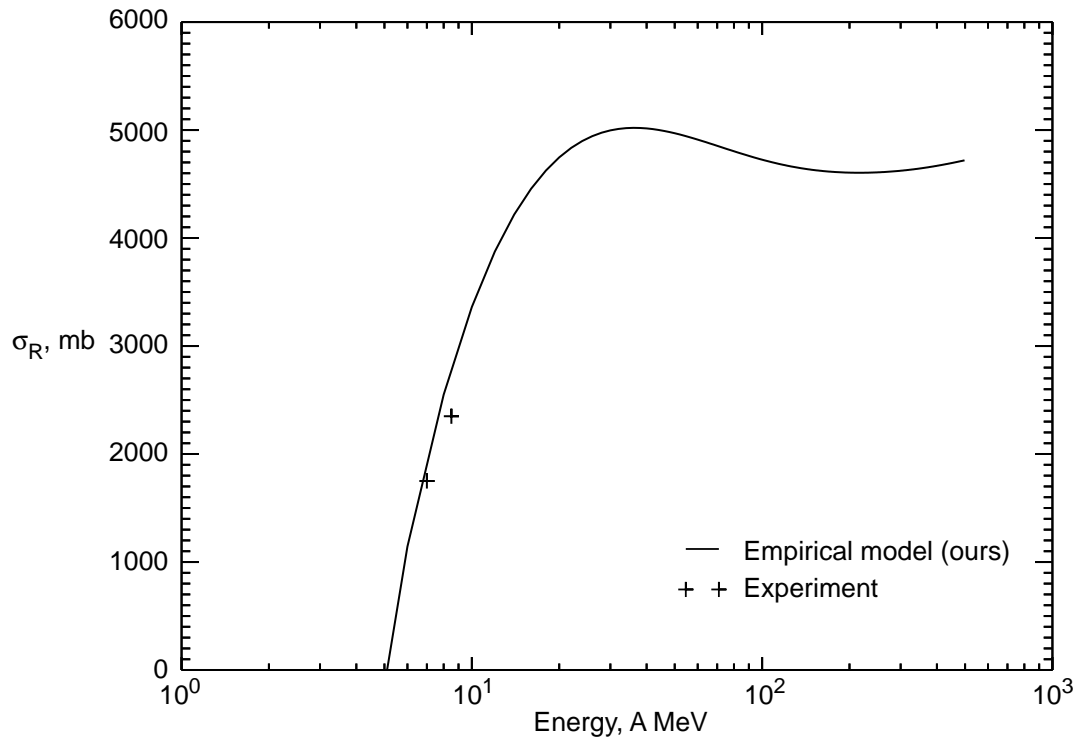


Figure 39. Reaction cross sections as a function of energy for $^{40}_{18}\text{Ar} + ^{238}_{92}\text{U}$ collisions.

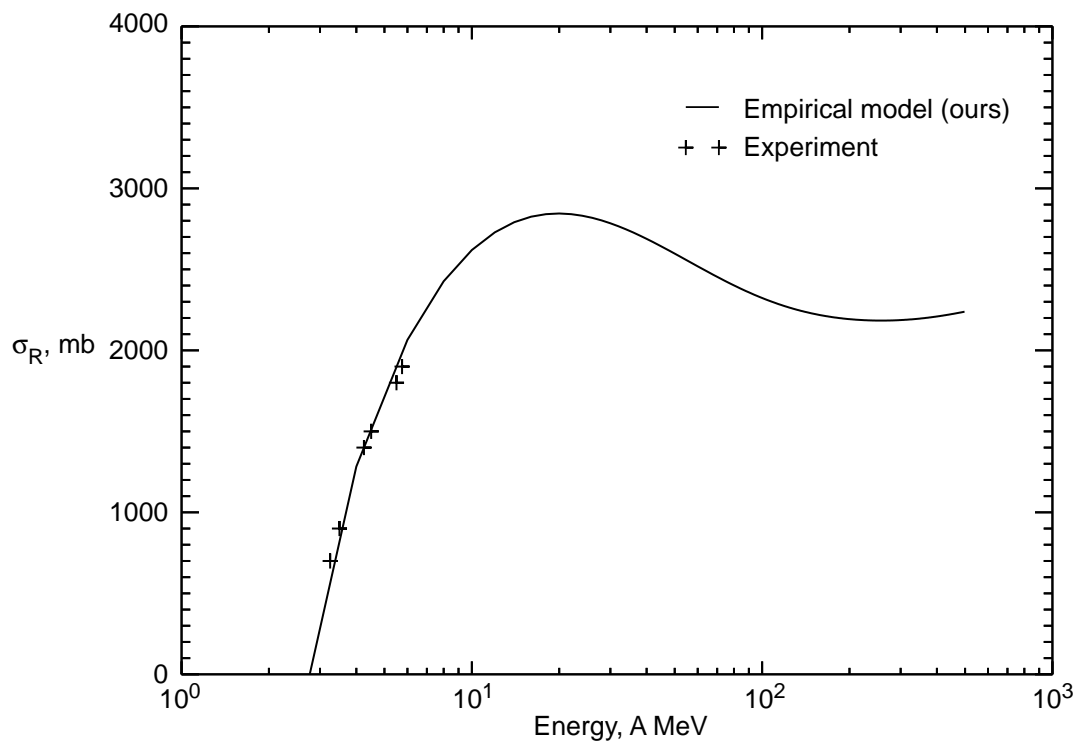


Figure 40. Reaction cross sections as a function of energy for $^{40}_{20}\text{Ca} + ^{40}_{20}\text{Ca}$ collisions.

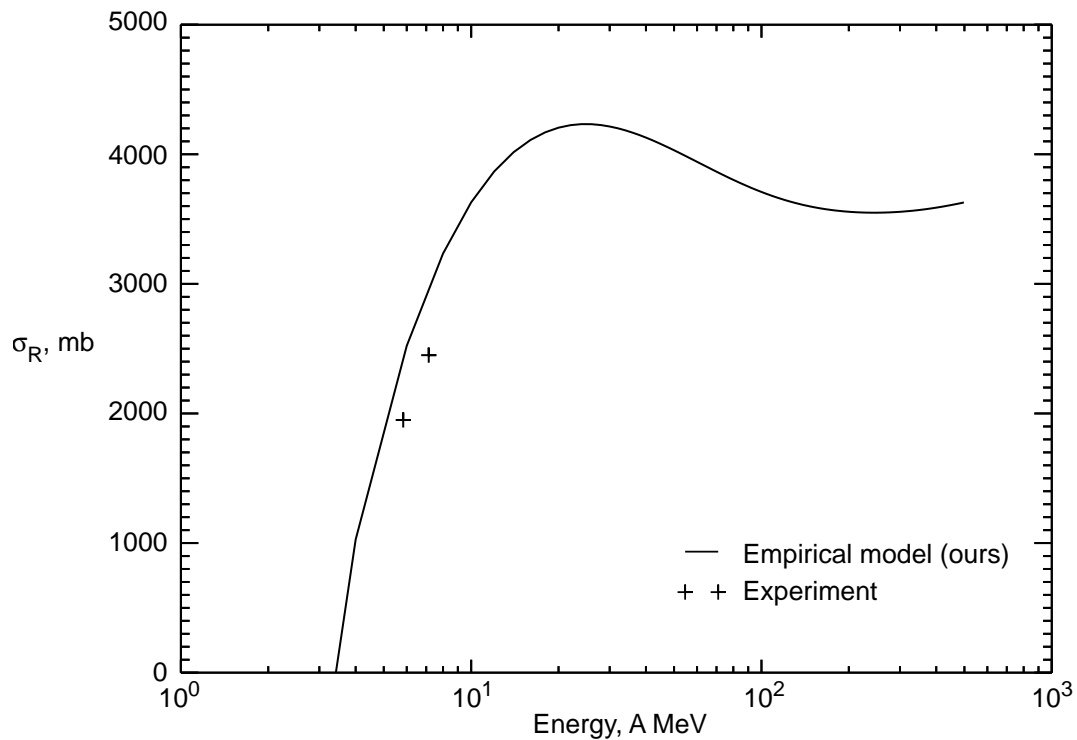


Figure 41. Reaction cross sections as a function of energy for $^{84}_{36}\text{Kr} + ^{65}_{29}\text{Cu}$ collisions.

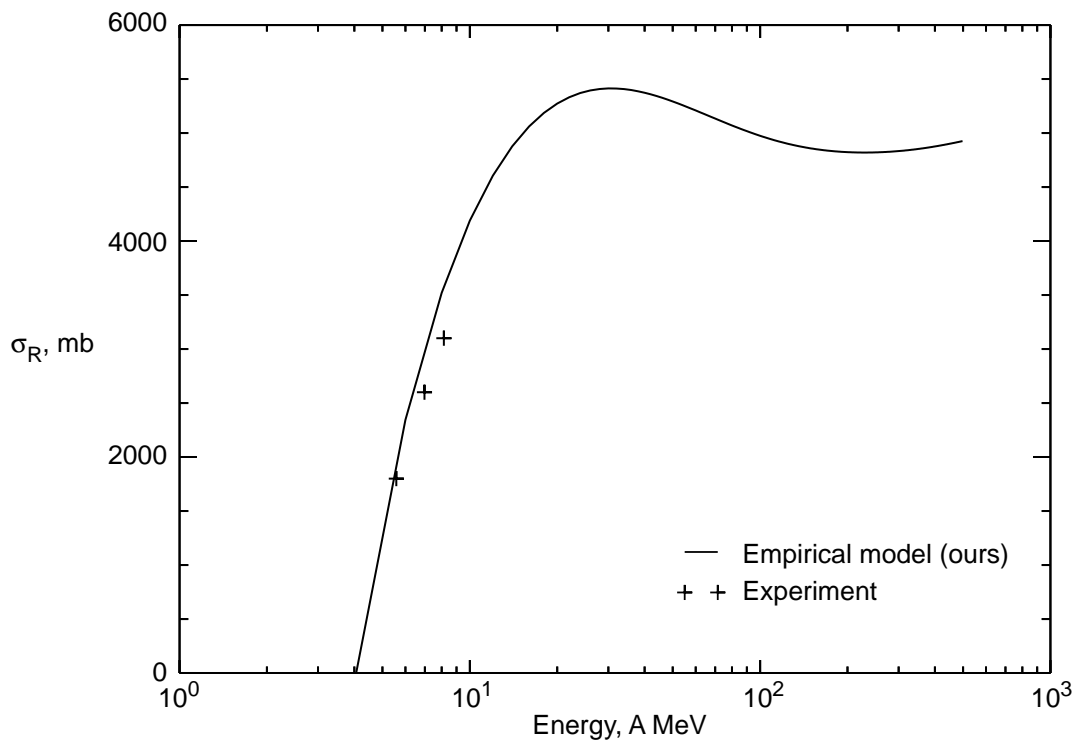


Figure 42. Reaction cross sections as a function of energy for $^{86}_{36}\text{Kr} + ^{139}_{57}\text{La}$ collisions.

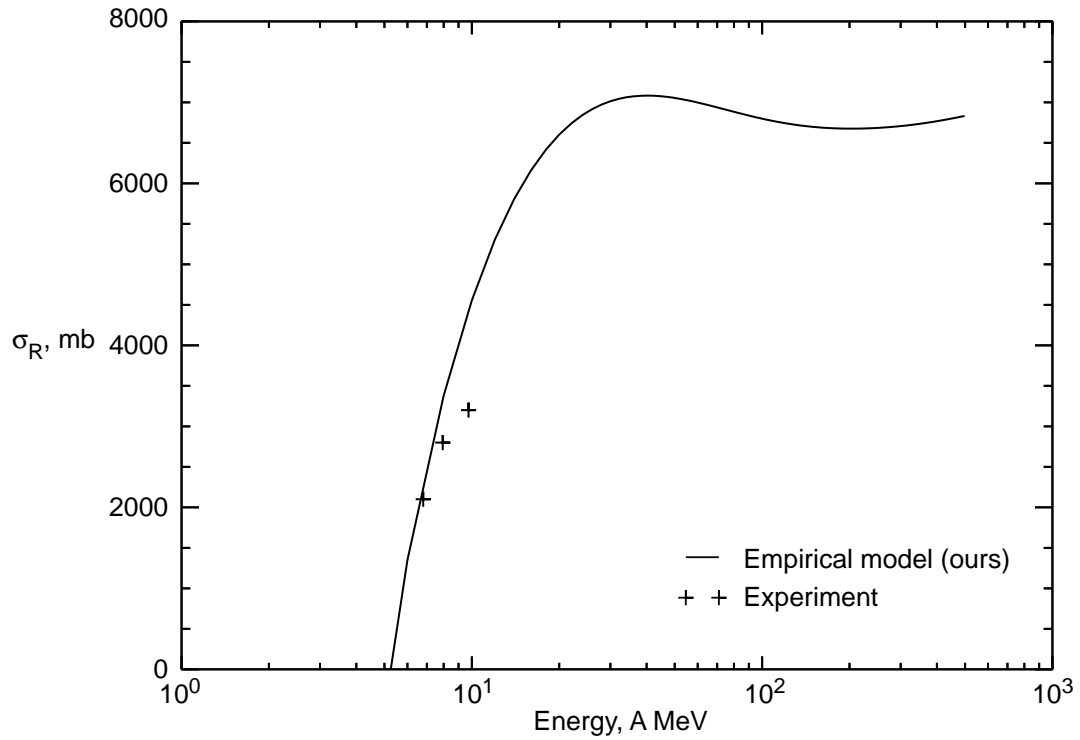


Figure 43. Reaction cross sections as a function of energy for $^{136}_{54}\text{Xe} + ^{209}_{83}\text{Bi}$ collisions.

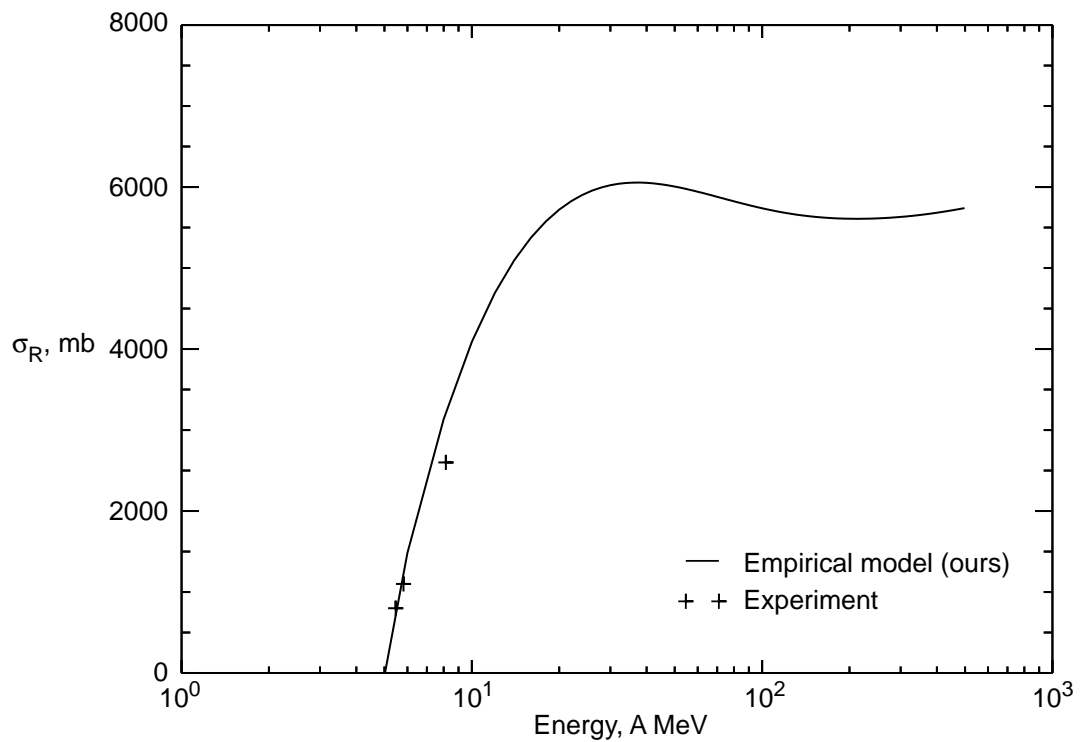


Figure 44. Reaction cross sections as a function of energy for $^{84}_{36}\text{Kr} + ^{208}_{82}\text{Pb}$ collisions.

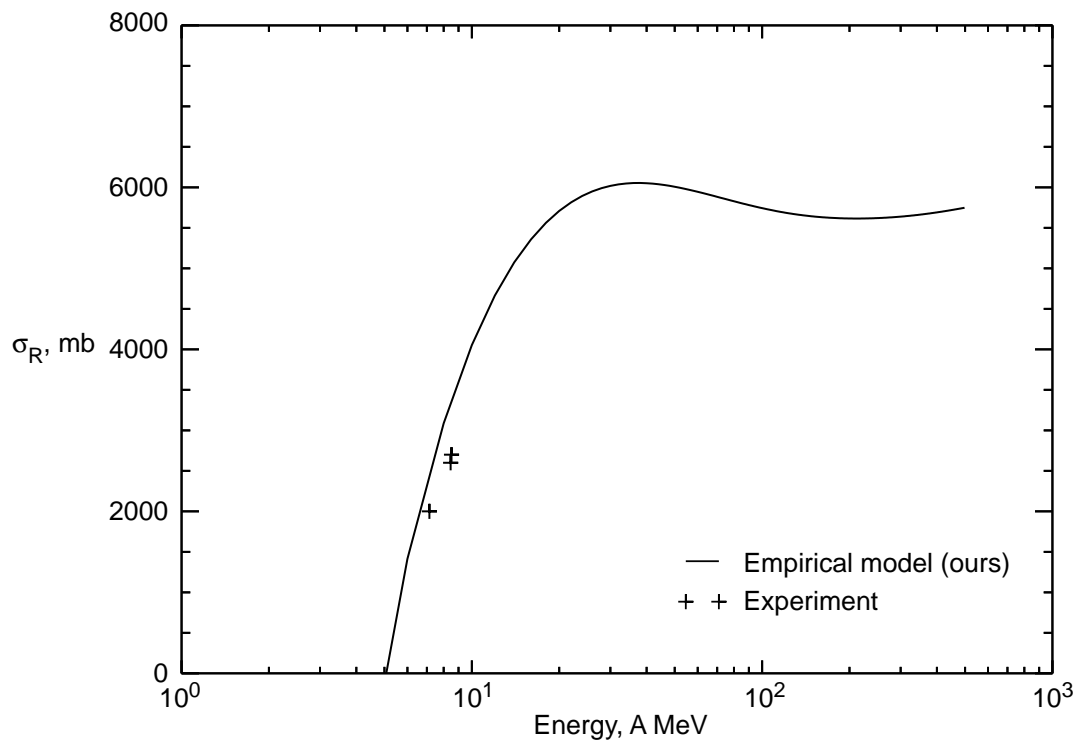


Figure 45. Reaction cross sections as a function of energy for $^{84}_{36}\text{Kr} + ^{209}_{83}\text{Bi}$ collisions.

REPORT DOCUMENTATION PAGE

Form Approved
OMB No. 0704-0188

Public reporting burden for this collection of information is estimated to average 1 hour per response, including the time for reviewing instructions, searching existing data sources, gathering and maintaining the data needed, and completing and reviewing the collection of information. Send comments regarding this burden estimate or any other aspect of this collection of information, including suggestions for reducing this burden, to Washington Headquarters Services, Directorate for Information Operations and Reports, 1215 Jefferson Davis Highway, Suite 1204, Arlington, VA 22202-4302, and to the Office of Management and Budget, Paperwork Reduction Project (0704-0188), Washington, DC 20503.

1. AGENCY USE ONLY <i>(Leave blank)</i>	2. REPORT DATE January 1997	3. REPORT TYPE AND DATES COVERED Technical Paper	
4. TITLE AND SUBTITLE Universal Parameterization of Absorption Cross Sections		5. FUNDING NUMBERS WU 199-45-16-11	
6. AUTHOR(S) R. K. Tripathi, Francis A. Cucinotta, and John W. Wilson			
7. PERFORMING ORGANIZATION NAME(S) AND ADDRESS(ES) NASA Langley Research Center Hampton, VA 23681-0001		8. PERFORMING ORGANIZATION REPORT NUMBER L-17580	
9. SPONSORING/MONITORING AGENCY NAME(S) AND ADDRESS(ES) National Aeronautics and Space Administration Washington, DC 20546-0001		10. SPONSORING/MONITORING AGENCY REPORT NUMBER NASA TP-3621	
11. SUPPLEMENTARY NOTES Tripathi: Southern Illinois University, Carbondale, IL; Cucinotta and Wilson: NASA Langley Research Center, Hampton, VA.			
12a. DISTRIBUTION/AVAILABILITY STATEMENT Unclassified-Unlimited Subject Category 93 Availability: NASA CASI (301) 621-0390		12b. DISTRIBUTION CODE	
13. ABSTRACT <i>(Maximum 200 words)</i> This paper presents a simple universal parameterization of total reaction cross sections for any system of colliding nuclei that is valid for the entire energy range from a few AMeV to a few AGeV. The universal picture presented here treats proton-nucleus collision as a special case of nucleus-nucleus collision, where the projectile has charge and mass number of one. The parameters are associated with the physics of the collision system. In general terms, Coulomb interaction modifies cross sections at lower energies, and the effects of Pauli blocking are important at higher energies. The agreement between the calculated and experimental data is better than all earlier published results.			
14. SUBJECT TERMS Nuclear reaction; Cross sections; Heavy ions		15. NUMBER OF PAGES 27	
		16. PRICE CODE A03	
17. SECURITY CLASSIFICATION OF REPORT Unclassified	18. SECURITY CLASSIFICATION OF THIS PAGE Unclassified	19. SECURITY CLASSIFICATION OF ABSTRACT Unclassified	20. LIMITATION OF ABSTRACT